A Potent and Site-Selective Agonist of TRPA1

Junichiro Takaya[†‡], Kazuhiro Mio[∥], Takuya Shiraishi[#], Tatsuki Kurokawa[#], Shinya Otsuka[§], Yasuo Mori[#⊥], and Motonari Uesugi*[‡§]

[†]Graduate School of Medicine, Kyoto University, Kyoto, Kyoto 606-8501, Japan [‡]Institute for Chemical Research and [§]Institute for Integrated Cell-Material Sciences (WPI-iCeMS), Kyoto University, Uji, Kyoto 611-0011, Japan [∥]Molecular Profiling Research Center for Drug Discovery, National Institute for Advanced Industrial Science and Technology, Koto-ku, Tokyo 135-0064, Japan [#]Department of Synthetic Chemistry and Biological Chemistry, Graduate School of Engineering and [⊥]Department of Technology and Ecology, Hall of Global Environment Studies, Kyoto University, Nishikyo-ku, Kyoto 615-8510, Japan

TRPA1, cation channel, chemical biology, chemical library, electron microscopy

ABSTRACT: TRPA1 is a member of the transient receptor potential (TRP) cation channel family that is expressed primarily on sensory neurons. This chemo-sensor is activated through covalent modification of multiple cysteine residues with a wide range of reactive compounds including allyl isothiocyanate (AITC), a spicy component of wasabi. The present study reports on potent and selective agonists of TRPA1, discovered through screening 1,657 electrophilic molecules. In an effort to validate the mode of action of hit molecules, we noted a new TRPA1-selective agonist, JT010 (molecule **1**), which opens the TRPA1 channel by covalently and site-selectively binding to Cys621 (EC_{50} = 0.65 nM). The results suggest that a single modification of Cys621 is sufficient to open the TRPA1 channel. The TRPA1-selective probe described herein might be useful for further mechanistic studies of TRPA1 activation.

■ INTRODUCTION

The transient receptor potential (TRP) channel superfamily comprises a diverse group of cation channels that mediate a variety of physiological processes.[1,2] Among the members, the TRPV1 and TRPA1 channels sense endogenous algesic substances and environmental irritants, evoking defensive responses, such as pain, coughing, and changes in respiration pattern.[3-6] Due to their involvement in nociception, TRPV1 and TRPA1 have been targets for the development of novel pain reducers.[7,8]

TRPA1 senses broader environmental stimuli than TRPV1, including cold,[9] abnormal pH,[10-13] zinc,[14] and reactive irritants.[15-17] The best recognized agonist of TRPA1 is allyl isothiocyanate (AITC), a spicy component of wasabi.[18] Electrophilic molecules, including AITC, react covalently with multiple cysteine residues of TRPA1, causing conformational change that opens the channel.[15,16] Site-directed mutagenesis studies have identified three cysteines within the cytoplasmic NH_2-terminus of human TRPA1 (Cys621, Cys641, and Cys665), whose simultaneous mutation negates the channel-activating effects of several electrophilic reagents.[15] On the other hand, mass spectrometric analysis has revealed three cysteines on mouse TRPA1 (Cys415, Cys422, and Cys622) as target sites for electrophilic agonists.[16] Those target sites are conserved in the human homolog of TRPA1 (Cys414, Cys421, and Cys621).

Despite these insights, it remains unclear how the modification of multiple cysteine residues leads to the activation of TRPA1. The present study reports the discovery and analysis of a new potent, TRPA1-selective agonist. JT010 (molecule **1**), a thiazole derivative equipped with a chloroacetyl group, binds covalently and selectively to a single cysteine, Cys621, to open the TRPA1 channel (EC_{50} = 0.65 nM). The site-selective chemical probe described herein might serve as a tool for further mechanistic studies of TRPA1 activation.

■ RESULTS

Screening of electrophilic molecules. TRPA1 is generally thought to be activated by reactive molecules, including electrophilic compounds. To identify potent, selective agonists of TRPA1, we screened a chemical library of 1,657 moderately electrophilic molecules that contain chloroacetyl, bromoacetyl, or epoxide groups (Figure S1A-D). The molecules were screened to identify agonists that cause a calcium influx in TRPA1-transfected HEK293 cells. The calcium influx was estimated by measuring signals from Fluo-8, a fluorescent Ca^{2+}-indicator dye. Three structurally-related molecules induced a calcium influx at half maximal effective concentrations (EC_{50}) less than 1 nM (Figure S1E). These hit molecules share a 2-chloro-*N*-(thiazol-2-yl)acetamide structure (Figure S1F). We selected one of the three molecules, 2-chloro-*N*-(4-(4-ethoxyphenyl)thiazol-2-yl)-*N*-(3-methoxypropyl)acetamide (JT010; molecule **1** in Figure 1A) for further investigation.

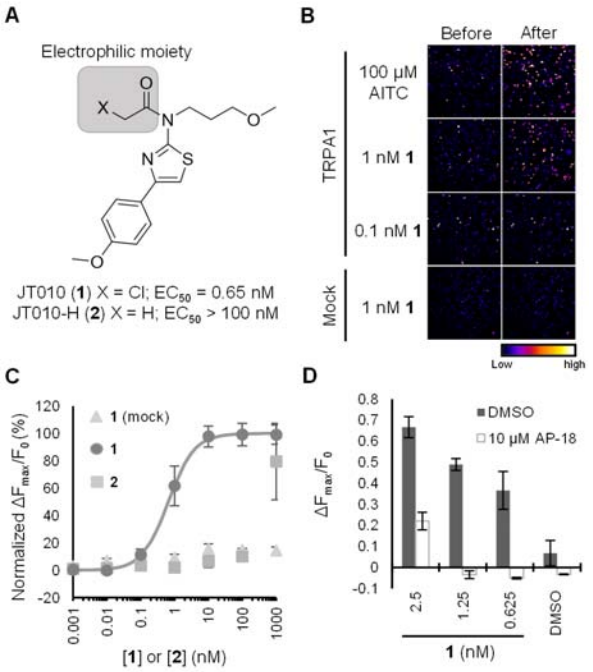

Figure 1. Molecule **1** stimulates calcium influx through the TRPA1 channel. (A) Chemical structures of JT010 (**1**) and its non-electrophilic derivative, JT010-H (**2**). (B) Representative calcium images analyzed for response of Fluo-8-loaded TRPA1- or mock-transfected HEK293 cells to molecule **1** or AITC. (C) Dose-response curve of Fluo-8 fluorescence changes induced by molecule **1** or **2** in TRPA1- or mock-transfected cells. Fluorescence changes ($\Delta F_{max}/F_0$) were normalized to the maximum response induced by molecule **1**. The plots were fitted to a four-parameter logistic model, using Image J. An EC_{50} of 0.65 nM was calculated from the fitted curve. Data points are mean ± s.e.m. (n = 3). (D) The inhibitory effect of AP-18 on Fluo-8 fluorescence changes induced by molecule **1** in TRPA1-transfected HEK293 cells. 10 μM AP-18 or DMSO (control) were added to the cells prior to activation of TRPA1 by molecule **1** at the various concentrations. Data points are mean ± s.d. (n = 2).

Molecule 1 as a potent electrophilic agonist of TRPA1. The chemical structure of molecule **1** was confirmed by its chemical synthesis (Scheme S1) and TRPA1 activity (Figure 1A-C). Calcium imaging assays demonstrated that 1 nM of synthesized molecule **1** caused calcium influx at comparable levels to 100 μM AITC in cells overexpressing TRPA1, but caused no detectable activity in the mock-transfected cells (Figure 1B). The effect of molecule **1** is dose-dependent, with an EC_{50} value of 0.65 nM (Figure 1C). In contrast, JT010-H (**2**), a derivative of molecule **1** in which Cl is replaced with H, displayed activity ~1000 times weaker (EC_{50} > 100 nM), indicating the importance of the electrophilic functional group of molecule **1**. It is likely that molecule **1** reacts with cysteine residues in TRPA1, similarly to other electrophilic agonists, including AITC.

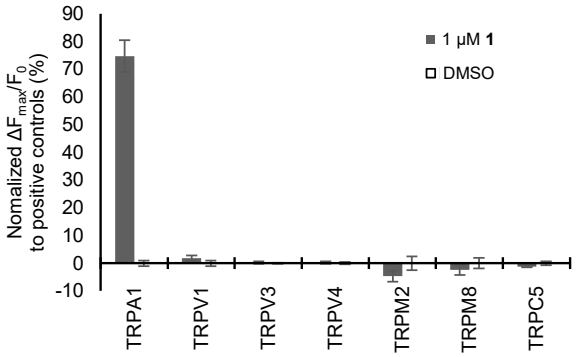

Figure 2. Among TRP channels, molecule **1** selectively affects TRPA1. Fluo-8 fluorescence changes stimulated by 1 μM molecule **1** or DMSO (control) in TRPA1-, TRPV1-, TRPV3-, TRPV4-, TRPM2-, TRPM8-, or TRPC5-transfected HEK293 cells. Fluorescence changes were normalized to the following positive controls: TRPA1 to 100 μM AITC; TRPV1 to 10 μM capsaicin; TRPV3 and TRPV4 to 50 μM 2-APB; TRPM2 to 1 mM H_2O_2; TRPM8 to 100 μM L-menthol; TRPC5 to 30 μM DTNP. Data points are mean ± s.e.m. (n = 3).

To confirm that the calcium influx activity of molecule **1** is TRPA1-dependent, we examined the effects of AP-18 and HC-030031, selective antagonists of TRPA1,[19,20] on the activity of molecule **1**. As expected, AP-18 (10 μM) suppressed calcium influx stimulated by molecule **1** in cells overexpressing TRPA1 (Figure 1D). The inhibitory effect of AP-18 and HC-030031 was dose-dependent, with IC_{50} values of 9.1 and 10.3 μM, respectively (Figure S2).

Selectivity of molecule 1 among TRP channels. Known TRPA1 agonists often activate TRP channels other than TRPA1. For example, SNAP, an NO donor, potentiates TRPA1, TRPV1, TRPV3, TRPV4, and TRPC5;[21,22] H_2O_2 stimulates TRPA1, TRPM2, and TRPC5;[23,24] L-menthol evokes TRPA1, TRPV3 and TRPM8;[25] and isothiocyanates, including AITC, activate TRPA1 and TRPV1.[26-28] Calcium imaging assays with HEK293 cells that express all seven of the selected TRP channels showed that molecule **1** is highly selective for TRPA1 (Figure 2). TRPV1, TRPV3, TRPV4, TRPM2, TRPM8, and TRPC5 were not activated, even with 1 μM of molecule **1**.

Covalent interaction of molecule 1 with TRPA1. To confirm the covalent interaction of molecule **1** with TRPA1, we chemically synthesized molecule **3,** a biotinylated analog of molecule **1** (Figure 3A, Scheme S2). Molecule **3** retained a nM-range activity (EC_{50} = 30 nM), although its activity was ~50 times weaker than that of molecule **1** (Figure 3B).

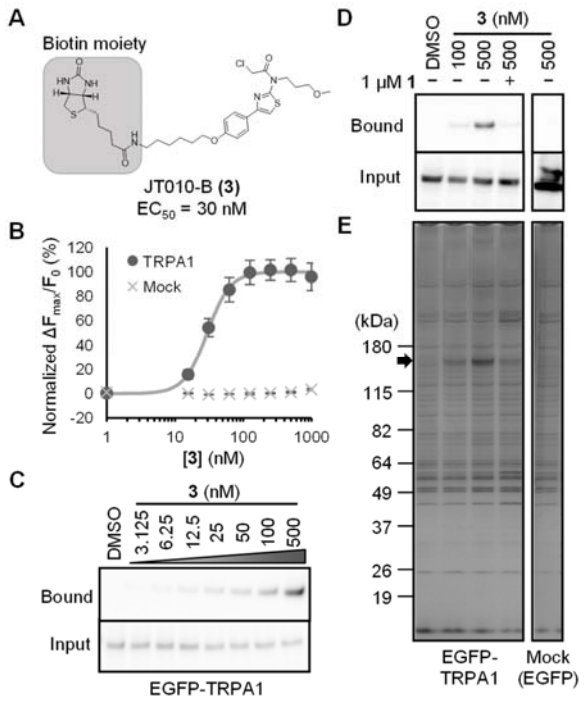

Figure 3. Selective biotinylation of TRPA1 by molecule **3**. (A) Chemical structure of molecule **3** (JT010-B), a biotinylated derivative of molecule **1**. (B) Dose-response curve for molecule **3**-induced Fluo-8 fluorescence changes in TRPA1- or mock-transfected cells. Fluorescence changes were normalized to the maximum response induced by molecule **3**. The plots were fitted to a four-parameter logistic model, using Image J. An EC_{50} value of 30 nM was calculated from the fitted curve. Data points are mean ± s.e.m. (n = 6-15). (C) Dose-dependent biotinylation of EGFP-TRPA1 by molecule **3**. EGFP-TRPA1-transfected HEK293 cells were incubated for 10 min with molecule **3** or DMSO (control) at various concentrations, and biotinylated proteins were purified using avidin beads. Purified samples (Bound) and cell lysate (Input) were analyzed by Western blot analysis with EGFP antibody. (D) Molecule **1** prevents biotinylation of EGFP-TRPA1 by molecule **3**. EGFP-TRPA1- or mock(EGFP)-transfected cells were treated with molecule **1** and/or **3** at the various conditions, and biotinylated proteins were purified and analyzed by Western blot analysis. (E) SDS-PAGE analysis with silver staining of an aliquot of the samples in D. Arrow indicates a single band at ~160 kDa that is dependent on molecule **3**.

Molecule **3** was incubated for 10 min with cells overexpressing TRPA1 fused with EGFP at the NH_2 terminus. After extensive wash, the cells were lysed, and the proteins that reacted with molecule **3** were purified using avidin agarose beads. Western blot analysis with an EGFP antibody visualized the biotinylated EGFP-TRPA1 in a dose-dependent manner (Figure 3C). When mock-transfected cells were used, no bands were detected. Moreover, competition

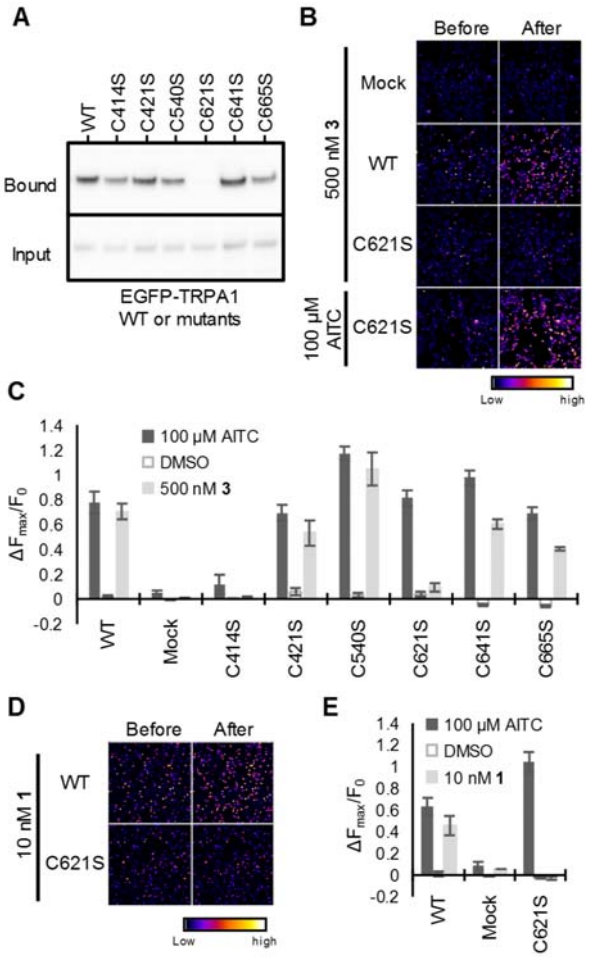

Figure 4. A TRPA1 C621S mutant resists both biotinylation and channel opening induced by molecule **3**. (A) Effect of Cys to Ser mutations. EGFP-TRPA1 wild type- (WT) or mutant-transfected (C414S, C421S, C540S, C621S, C641S or C665S) HEK293 cells were incubated with molecule **3** (500 nM), and biotinylated proteins were purified using avidin beads and analyzed by western blot analysis. (B) Representative calcium imaging for response analysis of Fluo-8-loaded WT-, C621S-, or mock-transfected HEK293 cells to molecule **3** or AITC. (C) Effect of the mutations on channel responses to molecule **3**, DMSO control, or AITC. Data points are mean ± s.e.m. (n = 3-20). (D) Representative calcium imaging for response analysis of Fluo-8-loaded WT- or C621S-transfectd HEK293 cells to molecule **1**. (E) Effect of the C621S mutant on channel responses to molecule **1**, DMSO control, or AITC. Data points are mean ± s.e.m. (n = 3-4).

with excess amounts of molecule **1** impaired the biotinylation of EGFP-TRPA1 (Figure 3D). When similar experiments were performed with an antibody against TRPA1 instead of the EGFP antibody, essentially the same results were obtained (Figure S3).

An aliquot of the samples was also analyzed by SDS-PAGE analysis, and the proteins in the gel were visualized

by silver staining (Figure 3E). Many bands were detected on the gel, possibly due to the presence of endogenous biotinylated proteins and non-specific proteins. However, we observed a single band at ~160 kDa that is dependent on molecule **3**, consistent with the size of the EGFP-TRPA1 fusion protein. The intensity of this band was reduced, when the cells were co-incubated with excess amounts of molecule **1**, or when mock-transfected cells were used.

To confirm the irreversible reaction of molecule **3** with TRPA1, we carried out another biotinylation experiment. Cells overexpressing EGFP-TRPA1 were pretreated with molecule **1** (50 nM) for 10 min. After extensive wash, the cells were incubated with molecule **3** (500 nM). Pretreatment with molecule **1** impaired the ability of molecule **3** to form a covalent bond with EGFP-TRPA1 (Figure S4). Pretreatment with molecule **2,** a non-electrophilic analog of molecule **1**, failed to do so, even at concentrations up to 5 μM (Figure S5). Furthermore, when the cells were pretreated with molecule **3** for 10 min and subsequently incubated with molecule **1**, we observed no detectable effects on the ability of molecule **3** to form a covalent bond with EGFP-TRPA1 (Figure S4). These results support our hypothesis that molecules **1** and **3** form irreversible bonds with EGFP-TRPA1.

The binding site of molecule 3. Pretreatment of cells overexpressing EGFP-TRPA1 with AITC, a TRPA1 agonist found in wasabi, also impaired the ability of molecule **3** to form a covalent bond with EGFP-TRPA1, although high concentrations (>25 μM) of AITC were required (Figure S6). This result suggests that the modification sites of molecule **3** overlap those of AITC.

The modification sites of electrophilic agonists, including AITC, have been identified as six cysteine residues in the NH_2 terminal cytosolic segment of TRPA1: Cys414, Cys421, Cys540, Cys621, Cys641, and Cys665.[15,16,21] Cells overexpressing EGFP fusions of TRPA1 mutants, in which one of the six cysteines was replaced with a serine, were incubated with molecule **3** (500 nM), and the effects were analyzed using western blots. The C621S mutant of TRPA1 was resistant to the modification; all other mutants reacted with molecule **3** at levels comparable to the wild type (Figure 4A). These results suggest that Cys621 is the major binding site of molecule **3**.

To confirm that Cys621 mediates the channel opening induced by molecule **3**, HEK293 cells overexpressing a C621S mutant of TRPA1 were treated with molecule **3**. As expected, the C621S mutant cells were almost completely nonresponsive to molecule **3**, even at 500 nM, while wild type cells exhibited calcium influx in the presence of the same concentration of molecule **3** (Figure 4B and S7). In contrast, the response of the C621S mutant cells to AICT was similar to that of the wild type cells.

Ser mutants of the five other cysteine residues were also examined in a cellular context (Figure 4C). Point mutations at Cys414 or Cys621 exhibited the most pronounced effects on channel opening induced by molecule **3**. Calcium

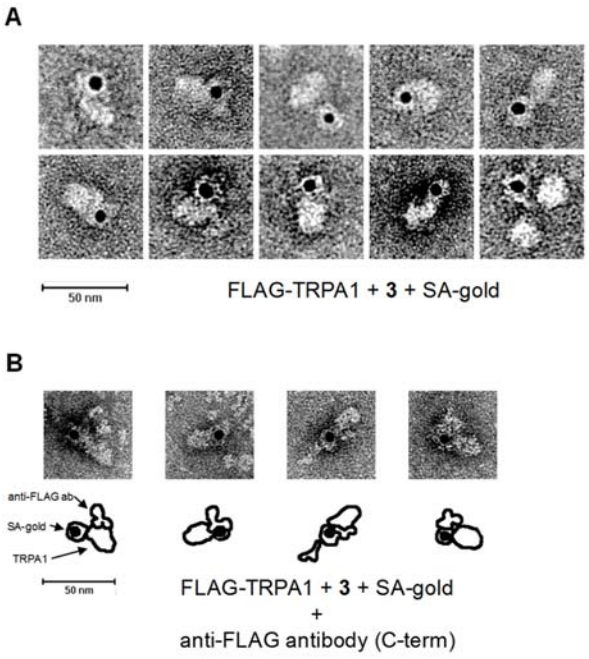

Figure 5. Electron microscopic observation of TRPA1 tetramer biotinylated by molecule **3**. (A) Representative negatively stained images of biotinylated FLAG-TRPA1 tetramer labeled with streptavidin-gold nanoparticle (SA-gold). Purified FLAG-TRPA1 tetramer was incubated with 5 μM molecule **3** for 1h and then labeled with SA-gold. (B) Estimated orientation of FLAG-TRPA1. The FLAG-tagged COOH terminal end of FLAG-TRPA1 is known to be cytoplasmic. The locations of the FLAG tags were estimated by adding an anti-FLAG antibody to the samples of (A).

influx levels of the C414S and C621S mutants in the presence of molecule **3** were as low as levels with DMSO, indicating that these two mutants were essentially nonresponsive to molecule **3**. However, the C414S mutant also exhibited little response to AITC. Presumably, Cys414 is generally required for opening the TRPA1 channel. In fact, Cys414 mutants have been shown to be nonresponsive even to 2-APB, a non-covalent TRPA1 agonist.[13,15,21]

When molecule **1** was similarly tested in the C621S mutant cells, molecule **1** (10 nM) failed to stimulate calcium influx in the C621S mutant cells, but induced calcium influx in the wild type cells (Figure 4D, E, and Figure S8). These results confirm that molecule **1** and **3** activates TRPA1 primarily through covalent modification at Cys621.

Direct observation of molecule 3 in TRPA1. Reactive TRPA1 agonists usually stimulate channel opening through modification of multiple cysteine residues.[16] The present study found that molecule **3** is a nM-range agonistic probe that opens the TRPA1 channel by binding covalently and selectively to a single cysteine, Cys621. The biotinylated chemical probe can be used as a tool for mechanistic studies of TRPA1.

To demonstrate its utility, we carried out electron microscopic visualization of the interaction between TRPA1 and molecule **3**. TRPA1 tagged with FLAG at the COOH terminus was overexpressed in FreeStyle™ 293-F cells, and purified through FLAG-affinity chromatography, wheat germ agglutinin (WGA) affinity chromatography, and size-exclusion chromatography (Figure S9A). Blue native-PAGE analysis showed a broad single band at ~560 kDa (Figure S9B), suggesting that purified FLAG-TRPA1 forms a tetramer, consistent with previously proposed models.[29,30]

The purified FLAG-TRPA1 tetramers were incubated with molecule **3** (5 μM) and streptavidin-gold conjugates (SA-gold). After removal of unreacted molecule **3** and SA-gold by FLAG-affinity chromatography, the biotinylation status of FLAG-TRPA1 was confirmed by avidin blot analysis, using streptavidin-HRP (Figure S10A). Electron microscopic observation of the negatively stained sample showed snowman-shaped images comprising two particles: a larger particle (FLAG-TRPA1) and a smaller particle (SA-gold). Comparison of the FLAG-TRPA1-particle images in the presence or absence of molecule **3** (Figure S10B) detected no obvious conformational transition of TRPA1 tetramers due to the relatively low resolution of the images. Based on the size of the black dots resulting from gold nanoparticles (5 nm), the FLAG-TRPA1 tetramer was estimated to be ~15 nm in diameter (Figure 5A, S10B), which agrees with previously proposed models.[30] Most of the SA-gold particles were located close to the end of the longer axis of the TRPA1 protein particles, suggesting the location of biotinylated sites in the particles.

To examine the orientation of FLAG-TRPA1 in the images, we treated the sample with an anti-FLAG antibody, which detects a FLAG tag at the cytoplasmic COOH terminus of FLAG-TRPA1 (Figure 5B). Preferred binding of anti-FLAG antibodies to the gold-labeled sides of particles suggested that the biotinylation sites are located in the cytoplasmic component of TRPA1. This observation is consistent with the proposed cytoplasmic location of Cys621.[29,30]

■ DISCUSSION

Results of the present study indicate that the chloroacetamide moiety of molecules **1** and **3** binds covalently and selectively to a single cysteine, Cys621, in TRPA1. The chloroacetamide group is generally known to be a moderately electrophilic functional group.[31] In fact, as high as >100 mM of dithiothreitol was required to prevent molecule **3** from reacting with TRPA1 in cells (Figure S11), and only 10% of molecule **1** reacted with 2-mercaptoethanol when incubated at the concentrations of 1 mM for 2 h (data not shown). Molecules **1** and **3** have a mechanism by which they react with Cys621 in TRPA1, in the presence of the abundant thiols and amines in cells.

During the course of our study, Paulsen *et al.* described a cryo-electron microscopic (Cryo-EM) structure of a TRPA1 tetramer, in which Cys621 is located at the NH_2 terminus of an α-helix and adjacent to a lysine.[30] The dipolar moment of the helix and the basicity of the lysine might reduce the pKa of the thiol moiety of Cys621, rendering Cys621 more nucleophilic than other cysteine residues. Furthermore, Cys621 is located in a pocket between an ankyrin repeat and an overlying helix-turn-helix. Presumably, the size and shape of the pocket are complementary to molecule **1**, increasing the reactivity of molecule **1** with Cys621 through proximity effects. In fact, the activity of molecule **1** is highly sensitive to modification. For example, screening of the chemical library revealed 73 molecules with a 2-chloro-*N*-(thiazol-2-yl)acetamide structure (Figure S1F), while only three of those molecules exhibited subnanomolar activity.

Three-dimensional structural analysis of a ligand-TRPA1 complex is needed for molecular understanding of how the modification of Cys621 with molecule **1** leads to opening of the TRPA1 channel. Such analysis was not possible in the recent Cryo-EM study, due to insufficient resolution of AITC-adducted TRPA1 and instability/inefficiency of the AITC adduct formation.[30] Molecule **1** (EC_{50} = 0.65 nM) is >3000-fold more potent than AITC (EC_{50} = 2 μM; Figure S6A). Molecule 1 might prove to be useful for future structural studies of a ligand–channel complex.

Our results suggest that Cys621 is important in channel opening. However, previous studies reported mixed results on the importance of Cys621. NNO-ABBH, a TRPA1-selective NO donor, retained its agonist activity in the C621S mutant,[21] while 15d-PGJ_2, an anti-inflammatory mediator known as the TRPA1 agonist,[32,33] exhibited suppressed channel opening and reduced binding with the C621S mutant.[13] Surprisingly, Moparthi *et al.* reported that a deletion mutant (Δ1-688 hTRPA1), lacking most of the cysteine residues that are important for electrophilic agonists, maintained its cold- and chemosensitivities.[34] Thus, modification of Cys621 is likely to be sufficient, but not necessary, for opening TRPA1 channel.

■ EXPERIMENTAL SECTION

Cell culture. Human embryonic kidney 293 (HEK293) cells were cultured in Dulbecco's modified Eagles' medium (Thermo Fisher Scientific Inc., Massachusetts, USA), containing 10% fetal bovine serum, 100 units/ml penicillin, 100 μg/ml streptomycin, and 0.25 μg/ml amphotericin B, at 37 °C under 5% CO_2.

Fluorescent calcium imaging with Fluo-8. Transfected cells were trypsinized, diluted with DMEM, and plated on poly-D-lysine-coated glass-bottom viewplate-96 F (PerkinElmer Inc., Waltham, MA, USA) at a density of 25,000-30,000 cells/well. Three to nine hours after plating, the medium was changed to flesh DMEM, containing 4 μM Fluo-8 AM (AAT Bioquest, Inc., Sunnyvale, CA, USA), and the cells were incubated at 37 °C under 5% CO_2 for 1 h. The medium containing Fluo-8 AM was replaced with 200 μL HEPES-buffered saline, containing the following: 107 mM

NaCl, 6 mM KCl, 1.2 mM $MgSO_4$, 2 mM $CaCl_2$, 11.5 mM glucose and 20 mM HEPES (pH 7.4, adjusted with NaOH). The Fluo-8 fluorescence images were recorded every 5 min, using Cell Voyager CV1000 (Yokogawa Electric Corporation, Tokyo, Japan), a confocal microscope system, with excitation by Ar laser (wavelength, 488 nm) and a 525/50 bandpass filter. Recorded images were analyzed using Image J (NIH, Bethesda, MD, USA)

Biotinylation assay. Transfected cells (3×10^6 cells plated on a 100 mm diameter dish) were collected by scraping and washed twice with PBS. The cells were divided into 8 tubes and mixed with or without molecule **3** and other chemicals at various concentrations. After extensive wash with PBS, the cell pellets were suspended in 1 mL RIPA buffer, containing the following: 150 mM NaCl, 1% Nonidet P-40, 1% sodium deoxycholate, 0.1% SDS in 25 mM Tris-HCl (pH 7.5), and 10 mM DTT with 1× protease inhibitor cocktail (Nacalai Tesque, Inc., Kyoto, Japan). The cell suspensions were sonicated using an ASTRASON W-385 ultrasonic processor (Heat Systems - Ultrasonics, Inc., Newtown, CT, USA) for 10 sec, and incubated on ice for 30 min. Lysates were centrifuged at 20,000 ×g for 20 min, and small portions of supernatants were collected as input fractions. Remaining supernatants were mixed with 25 µL of High Capacity NeutrAvidin Agarose Resin (Pierce Biotechnology, Waltham, MA, USA) or SoftLink™ Soft Release Avidin Resin (Promega Corp., Madison, WI, USA), and incubated at 4°C for 2-4 h. The resin was washed at least four times with RIPA buffer, and biotinylated samples were eluted from the beads. The High Capacity NeutrAvidin Agarose Resin was incubated with 1× SDS sample buffer, containing 100 mM DTT, at room temperature (RT) for 30 min. The SoftLink™ Soft Release Avidin Resin was incubated with RIPA buffer, containing 5 mM biotin at RT for 30 min. Eluted samples were collected as the bound fractions and examined by SDS-PAGE analysis in a 4-20% gradient gel (Cosmo Bio, Inc., Tokyo, Japan), and western blot analysis with Living Colors® EGFP Monoclonal Antibody (Clontech Laboratories, Inc., Palo Alto, CA, USA) or an anti-TRPA1 antibody (NB110-40763; Novus Biologicals, LLC, Littleton, CO, USA) diluted with Can Get Signal® Immunoreaction Enhancer Solution (Toyobo, Osaka, Japan). The blotted membranes were visualized with ECL Prime Western Blotting Detection Reagent and recorded using ImageQuant LAS500 (GE Healthcare, Little Chalfont, UK).

Electron Microscopic Analysis. Purified FLAG-TRPA1 tetramer was incubated with 5 µM molecule **3** at 4°C for 1 h. The sample was then incubated with 20 µL of anti-FLAG affinity beads (Sigma-Aldrich) for 1 h. After extensive wash, the beads were incubated with 4 µl of streptavidin-gold nanoparticle conjugate (BBInternational) at 4°C for 20 min. Unbound SA-gold conjugates were removed by washing the gel. The TRPA1-molecule **3**-SA-gold complex was eluted from the gel with 40 µl of 100 µg/ml FLAG peptide (Sigma-Aldrich). Peptide was removed by Superdex 200 gel filtration chromatography (GE Healthcare) prior to conjugation with anti-FLAG antibodies.

The eluate containing gold-labeled TRPA1 was adsorbed onto thin carbon films supported by copper mesh grids, which were rendered hydrophilic in advance by glow-discharge under low air pressure. Samples were washed with five drops of double-distilled water, negatively stained with 2% uranyl acetate solution for 30 sec twice, blotted, and dried in air. Samples were observed using a JEM1230 transmission electron microscope (JEOL, Tokyo, Japan) at × 60,000 magnification with 100 kV acceleration voltages. Images were recorded using a TVIPS F114T CCD camera (TVIPS, Oslo, Norway).

ASSOCIATED CONTENT

Supplemental information includes details on construction of recombinant plasmids, overexpression of recombinant proteins, chemical screening, quantification of Fluo8 fluorescence images, protein purification, synthesis schemes, and molecule characterization data including ^{1}H-NMR spectra.

This material is available free of charge via the Internet at http://pubs.acs.org.

AUTHOR INFORMATION

Corresponding Author

*uesugi@scl.kyoto-u.ac.jp

Notes

The authors declare no competing financial interest.

ACKNOWLEDGMENT

We thank N. Takahashi and D. Kozai for experimental support. This work was supported in part by JSPS KAKENHI Grant Number 26102728 and 26220206 (M.U.). iCeMS is supported by World Premier International Research Center Initiative (WPI), MEXT, Japan. This work was inspired by the international and interdisciplinary environments of the iCeMS and JSPS Asian CORE Program, "Asian Chemical Biology Initiative."

ABBREVIATIONS

AITC, Allyl isothiocyanate; AP-18, 4-(4-chlorophenyl)-3-methylbut-3-en-2-one oxime; 2-APB, 2-aminoethoxydiphenyl borate; DMSO, Dimethyl sulfoxide; DTNP, 2,2'-dithiobis(5-nitropyridine); HC-030031, 2-(1,3-dimethyl-2,6-dioxo-1,2,3,6-tetrahydro-7*H*-purin-7-yl)-*N*-(4-isopropylphenyl)acetamide; SNAP, *S*-nitroso-*N*-acetylpenicillamine; TRP, Transient receptor potential

REFERENCES

(1) Clapham, D. *Nature* **2003**, *426* (6966), 517-24.
(2) Nilius, B.; Owsianik, G.; Voets, T.; Peters, J. *Physiol. Rev.* **2007**, *87* (1), 165-217.
(3) Benemei, S.; Patacchini, R.; Trevisani, M.; Geppetti, P. *Curr. Opin. Pharmacol.* **2015**, *22*, 18-23.
(4) Bessac, B. F.; Sivula, M.; Hehn, C. A. von; Escalera, J.; Cohn, L.; Jordt, S.-E. E. *J. Clin. Invest.* **2008**, *118* (5), 1899-910.
(5) Bessac, B. F.; Jordt, S.-E. E. *Physiology (Bethesda)* **2008**, *23*, 360-70.
(6) Caterina, M. J.; Schumacher, M. A.; Tominaga, M.; Rosen, T. A.; Levine, J. D.; Julius, D. *Nature* **1997**, *389* (6653), 816-24.
(7) Moran, M.; McAlexander, M.; Bíró, T.; Szallasi, A. *Nat. Rev. Drug Discovery* **2011**, *10*, 601-620.

(8) Julius, D. *Annu. Rev. Cell Dev. Biol.* **2013**. 29: 355–84.
(9) Story, G. M.; Peier, A. M.; Reeve, A. J.; Eid, S. R.; Mosbacher, J.; Hricik, T. R.; Earley, T. J.; Hergarden, A. C.; Andersson, D. A.; Hwang, S. W.; McIntyre, P.; Jegla, T.; Bevan, S.; Patapoutian, A. *Cell* **2003**, *112* (6), 819-29.
(10) Wang, Y.; Chang, R.; Allgood, S.; Silver, W.; Liman, E. *J. Gen. Physiol.* **2011**, *137* (6), 493-505.
(11) Fujita, F.; Uchida, K.; Moriyama, T.; Shima, A.; Shibasaki, K.; Inada, H.; Sokabe, T.; Tominaga, M. *J. Clin. Invest.* **2008**, *118* (12), 4049-4057.
(12) Roche, J. de la; Eberhardt, M.; Klinger, A.; Stanslowsky, N.; Wegner, F.; Koppert, W.; Reeh, P.; Lampert, A.; Fischer, M.; Leffler, A. *J. Biol. Chem.* **2013**, *288* (28), 20280-20292.
(13) Takahashi, N.; Mizuno, Y.; Kozai, D.; Yamamoto, S.; Kiyonaka, S.; Shibata, T.; Uchida, K.; Mori, Y. *Channels* **2008**, *2* (4), 287-98.
(14) Hu, H.; Bandell, M.; Petrus, M.; Zhu, M.; Patapoutian, A. *Nat. Chem. Biol.* **2009**, *5* (3), 183-90.
(15) Hinman, A.; Chuang, H.; Bautista, D.; Julius, D. *Proc. Natl. Acad. Sci. U. S. A.* **2006**, *103* (51), 19564-19568.
(16) Macpherson, L.; Dubin, A.; Evans, M.; Marr, F.; Schultz, P.; Cravatt, B.; Patapoutian, A. *Nature* **2007**, *445* (7127), 541-5.
(17) Bautista, D.; Movahed, P.; Hinman, A.; Axelsson, H.; Sterner, O.; Högestätt, E.; Julius, D.; Jordt, S.-E.; Zygmunt, P. *Proc. Natl. Acad. Sci. U. S. A.* **2005**, *102* (34), 12248-12252.
(18) Jordt, S.-E. E.; Bautista, D. M.; Chuang, H.-H. H.; McKemy, D. D.; Zygmunt, P. M.; Högestätt, E. D.; Meng, I. D.; Julius, D. *Nature* **2004**, *427* (6971), 260-5.
(19) Petrus, M.; Peier, A.; Bandell, M.; Hwang, S.; Huynh, T.; Olney, N.; Jegla, T.; Patapoutian, A. *Mol. Pain* **2007**, *3*, 40.
(20) McNamara, C.; Mandel-Brehm, J.; Bautista, D.; Siemens, J.; Deranian, K.; Zhao, M.; Hayward, N.; Chong, J.; Julius, D.; Moran, M. *Proc. Natl. Acad. Sci. U. S. A.* **2007**, *104* (33), 13525-13530.
(21) Kozai, D.; Kabasawa, Y.; Ebert, M.; Kiyonaka, S.; Firman; Otani, Y.; Numata, T.; Takahashi, N.; Mori, Y.; Ohwada, T. *Mol. Pharmacol.* **2014**, *85*, 175-185.
(22) Yoshida, T.; Inoue, R.; Morii, T.; Takahashi, N.; Yamamoto, S.; Hara, Y.; Tominaga, M.; Shimizu, S.; Sato, Y.; Mori, Y. *Nat. Chem. Biol.* **2006**, *2* (11), 596-607.
(23) Sawada, Y.; Hosokawa, H.; Matsumura, K.; Kobayashi, S. *Eur. J. Neurosci.* **2008**, *27* (5), 1131-42.
(24) Hara, Y.; Wakamori, M.; Ishii, M.; Maeno, E.; Nishida, M.; Yoshida, T.; Yamada, H.; Shimizu, S.; Mori, E.; Kudoh, J.; Shimizu, N.; Kurose, H.; Okada, Y.; Imoto, K.; Mori, Y. *Mol. Cell* **2002**, *9* (1), 163-173.
(25) Macpherson, L. J.; Hwang, S. W.; Miyamoto, T.; Dubin, A. E.; Patapoutian, A.; Story, G. M. *Mol. Cell. Neurosci.* **2006**, *32* (4), 335-43.
(26) Everaerts, W.; Gees, M.; Alpizar, Y.; Farre, R.; Leten, C.; Apetrei, A.; Dewachter, I.; Leuven, F. van; Vennekens, R.; Ridder, D.; Nilius, B.; Voets, T.; Talavera, K. *Curr. Biol.* **2011**, *21* (4), 316-321.
(27) Uchida, K.; Miura, Y.; Nagai, M.; Tominaga, M. *Chem. Senses* **2012**, *37* (9), 809-818.
(28) Terada, Y.; Masuda, H.; Watanabe, T. *J. Nat. Prod.* **2015**, *78* (8), 1937-41.
(29) Cvetkov, T.; Huynh, K.; Cohen, M.; Moiseenkova-Bell, V. *J. Biol. Chem.* **2011**, *286* (44), 38168-38176.
(30) Paulsen, C. E.; Armache, J.-P. P.; Gao, Y.; Cheng, Y.; Julius, D. *Nature* **2015**, *520* (7548), 511-7.
(31) Weerapana, E.; Simon, G.; Cravatt, B. *Nat. Chem. Biol.* **2008**, *4*, 405-407.
(32) Taylor-Clark, T.; Undem, B.; Macglashan, D.; Ghatta, S.; Carr, M.; McAlexander, M. *Mol. Pharmacol.* **2007**, *73* (2), 274-281.
(33) Cruz-Orengo, L.; Dhaka, A.; Heuermann, R.; Young, T.; Montana, M.; Cavanaugh, E.; Kim, D.; Story, G. *Mol. Pain* **2008**, *4*, 30.
(34) Moparthi, L.; Survery, S.; Kreir, M.; Simonsen, C.; Kjellbom, P.; Högestätt, E.; Johanson, U.; Zygmunt, P. *Proc. Natl. Acad. Sci. U. S. A.* **2014**, *111* (47), 16901-16906.

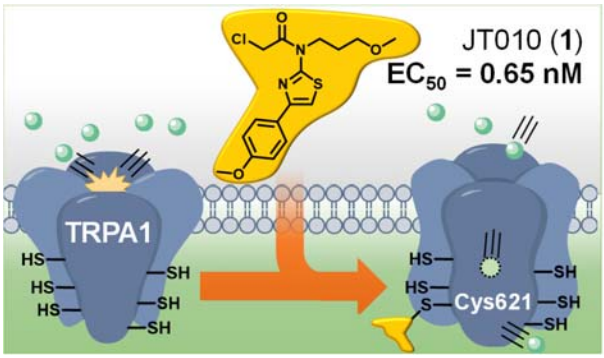

For Table of Contents Only

Supporting information

A Potent and Site-Selective Agonist of TRPA1

Junichiro Takaya, Kazuhiro Mio, Takuya Shiraishi, Tatsuki Kurokawa, Shinya Otsuka, Yasuo Mori and Motonari Uesugi*

The chemical library and the experimental reagents.

All compounds in the chemical library were purchased from the following sources; AMRI hungary, ASINEX, AnalytiCon Discovery, BIONET, Butt Park, Labotest, Life chemicals, Peakdale, Princeton, MDD, OTAVA, Pharmeks, Enamine, Scientific Exchange, TOSLab, Vitas-M, and TimTec. Other chemicals which used in the experiments were purchased from the following sources: 2-aminoethoxydiphenyl borate (2-APB) and 2,2'-dithiobis(5-nitropyridine) (DTNP) were purchased from Sigma-Aldrich Co. LLC. (St. Louis, MO, USA). Allyl isothiocyanate (AITC), capsaicin, and H_2O_2 were purchased from Wako Pure Chemical Industries Ltd. (Osaka, Japan). L-menthol and dithiothreitol (DTT) were purchased from Nacalai Tesque, Inc. (Kyoto, Japan). 4-(4-chlorophenyl)-3-methylbut-3-en-2-one oxime (AP-18) was purchased from R&D systems Inc. (Minneapolis, MN, USA). 2-(1,3-dimethyl-2,6-dioxo-1,2,3,6-tetrahydro-7*H*-purin-7-yl)-*N*-(4-isopropylphenyl)acetamide (HC-030031) was purchased from FOCUS biomolecules (Plymouth Meeting, PA, USA). 1-Acetoxy-3chloroacetone was purchased from Tokyo Chemical Industry Co., Ltd. (Tokyo, Japan). Fluo-8 AM was purchased from AAT Bioquest (Sunnyvale, CA, USA).

Construction of recombinant plasmids

The cDNA of human TRPA1 was inserted in pCI-neo (Promega Corp., Madison, WI, USA), pEGFP-C (Clontech Laboratories, Palo Alto, CA, USA), and pCMV-Tag 4 (Stratagene, La Jolla, CA, USA). Cys to Ser mutants of TRPA1, C414S, C421S, C540S, C621S, C641S, and C665S, were constructed using site-directed mutagenesis as previously reported.[1] As an exception, EGFP-C621S mutant was produced from a pEGFP-C construct of wildtype TRPA1 using a PrimeSTAR™ mutagenesis basal kit (Takara Bio, Inc., Shiga, Japan) with the following primers: 5'-AATAAAAGTCCAATTACAGAAATGATA-3' and 5'-AATTGGACTTTTATTGCCTGGAGAATT-3'. The sequence of the EGFP-C621S mutant was verified by sequencing (Data not shown), with two different primers: 5'-GCTTCTTCTGAGCCACAATG-3' and 5'-CACACAGGATGATTGAGAAGC-3'. Plasmids carrying TRPV1, TRPV3, TRPV4, TRPM2 and TRPC5 cDNAs were used as previously described.[2] Human TRPM8 was cloned from Human fetal lung, whole Marathon-Ready cDNA (Clontech Laboratories, Palo Alto, CA, USA) by applying a PCR-based approach. The TRP cDNAs were inserted in pCI-neo.

Overexpression of recombinant proteins.

HEK293 cells were transfected with recombinant plasmids using SuperFect Transfection Reagent (QIAGEN, Valencia, CA, USA) or polyethyleneimine (MW 40,000; Polysciences, Inc., Warrington, PA, USA). The SuperFect reagent was used according to the manufacturer's instructions. Polyethyleneimine was used at the concentration of 1.5 μg/mL in 10 mL DMEM with 5 μg plasmid DNA. Transfected cells were incubated at 37 °C under 5% CO_2 for 24-48 hours before used for the experiments.

Screening.

The chemical library of 1,657 electrophiles was screened with TRPA1-overexpressigng HEK293 cells by monitoring fluorescence signals from Fluo-8. The initial screening was carried out at the concentration of 100 nM of the chemical library members. Hit compounds were subsequently tested at lower concentrations (10 or 1 nM). The maximum fluorescence changes were normalized to the positive control, 1-acetoxy-3-chloroacetate (SI1; 1 μM).

Fluorescence calcium imaging with Fura-2.

Transfected cells were trypsinized and diluted by DMEM before plating on poly-L-lysine-coated glass coverslips. Three-nine hours after plating, the cells were incubated with 1 μM Fura-2 (Dojindo Labolatories, Kumamoto, Japan) for 30 min. Fura-2 fluorescence was measured in a HEPES-buffered saline containing the following: 107 mM NaCl, 6 mM KCl, 1.2 mM $MgSO_4$, 2mM CaCl2, 11.5 mM glucose and 20 mM HEPES (pH 7.4 adjusted with NaOH). The Fura-2 fluorescence images were analyzed with a video image analysis system AQUACOSMOS (Hamamtsu Photonics, Shizuoka, Japan), according to the manufacturer's instructions. The F_{340}/F_{380} ratios were obtained on a pixel-by pixel basis.

Quantification of Fluo-8 fluorescence images.

All quantifications were performed using an image J software (NIH). The maximum intensity projection (MIP) images were produced from the recorded images. An area of the cells in the MIP images was automatically selected by a threshold tool function. Average fluorescence intensities of the selected areas of the recorded images were quantified by a measurement tool function. The basal fluorescence intensity prior to adding compounds was defined as F_0. The maximum fluorescence intensity induced by compounds was defined as F_{max}.

Protein purification.

FreeStyle™ HEK293-F cells expressing TRPA1-FLAG (~ 4×10^8) were lysed by a homogenizer in 30 mL buffer A (TBS containing 25 mM *n*-dodecyl β-D-maltoside (DDM) (Sigma), 300 mM $MgCl_2$, 10% glycerol, protease inhibitors, and 0.02% sodium azide). After centrifuging at 100,000 ×g for 30 min, the supernatant containing solubilized TRPA1-FLAG was loaded onto 1 mL of an anti-FLAG affinity gel (Sigma). After extensive wash with 6 mL buffer B (TBS containing 1 mM DDM, 300 mM $MgCl_2$, 10% glycerol and 0.02% sodium azide), the bound TRPA1-FLAG protein was eluted with buffer B containing 125 μg/ml FLAG peptide (Sigma-Aldrich). The eluates were analyzed by SDS-PAGE followed by silver staining.

The TRPA1-FLAG-containing fractions were pooled and loaded onto 0.5 mL of the wheat germ agglutinin (WGA)-agarose (Seikagaku, Tokyo, Japan). After extensive wash with 1.5 mL buffer B, the bound TRPA1-FLAG protein was eluted by 3 mL buffer B containing 100 mM GlcNAc. The eluate was monitored by SDS-PAGE analysis. The TRPA1-FLAG-rich fractions were pooled, concentrated with a Microcon filter unit (YM-100; Millipore), and further purified by Superdex 200 size exclusion chromatography (SEC) in a SMART System (GE Healthcare) using buffer B. The elution of proteins from the SEC was monitored by UV absorbance at 280 nm and SDS-PAGE analysis.

References

(1) Kozai, D.; Kabasawa, Y.; Ebert, M.; Kiyonaka, S.; Firman; Otani, Y.; Numata, T.; Takahashi, N.; Mori, Y.; Ohwada, T. *Mol. Pharmacol.* **2014**, *85* (1), 175-185.

(2) Takahashi, N.; Kuwaki, T.; Kiyonaka, S.; Numata, T.; Kozai, D.; Mizuno, Y.; Yamamoto, S.; Naito, S.; Knevels, E.; Carmeliet, P.; Oga, T.; Kaneko, S.; Suga, S.; Nokami, T.; Yoshida, J.; Mori, Y. *Nat. Chem. Biol.* **2011**, *7*, 701-711.

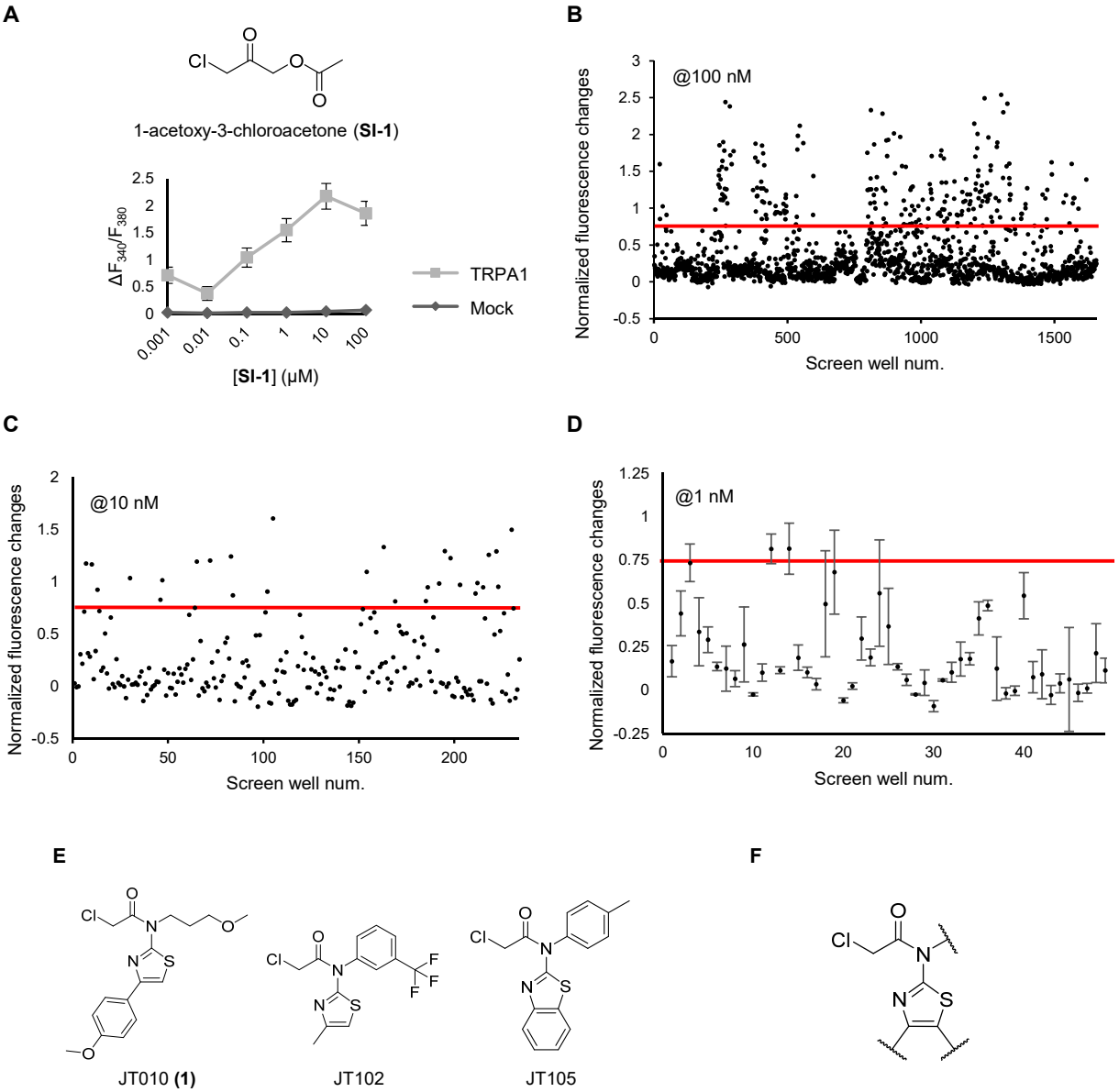

Figure S1. Screening for TRPA1 agonists. (A) Dose-response curves for Fura-2 fluorescence ratio changes ($\Delta F_{340}/F_{380}$) induced by 1-acetoxy-3-chloroacetone (**SI-1**) in TRPA1- or mock-transfected HEK293 cells. Data points are mean ± s.e.m. (n = 23-42). (B-D) Fluo-8 fluorescence changes in TRPA1-transfected cells evoked by compounds in the chemical library at the concentrations of 100, 10, 1 nM. Fluorescence changes were normalized to the response evoked by 1 μM **SI-1**. Molecules with values over 0.75 (red bar) were selected as hit molecules. Data points in D are mean ± s.e.m. (n = 3). (E) Chemical structures of structurally related hit molecules, JT010 (**1**), JT102 and JT105. (F) Shared structure of the hit molecules.

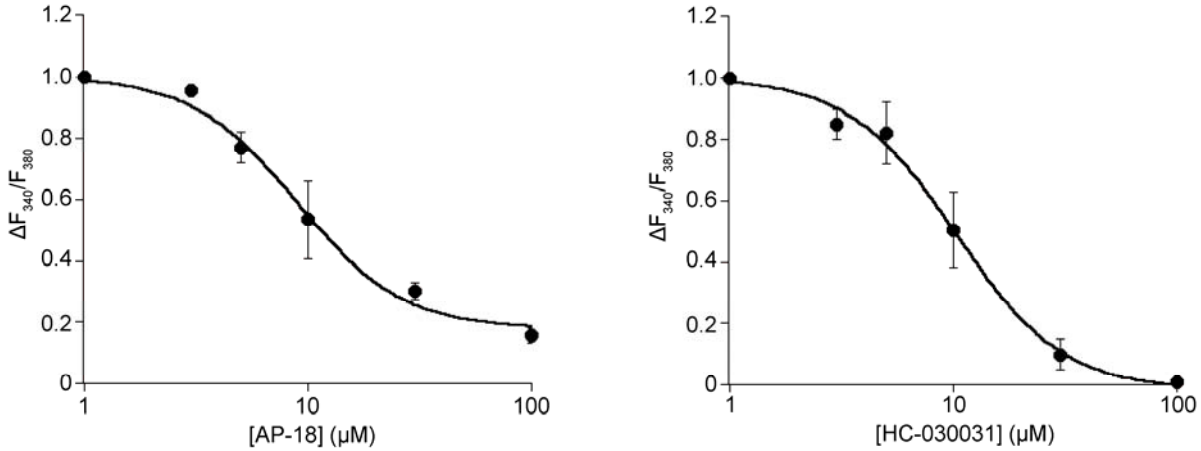

Figure S2. Dose-dependent inhibitory effects of AP-18 and HC-030031 on Fura-2 fluorescence ratio changes ($\Delta F_{340}/F_{380}$) induced by 30 nM molecule **1** in TRPA1-transfected HEK293 cells. The antagonists were added at the various concentrations to the cells prior to the activation of TRPA1 by molecule **1** (30 nM). The plots were fitted to a four parameter logistic model using KaleidaGraph. IC_{50} values of AP-18 and HC-030031 were calculated to be 9.1 and 10.3 μM, respectively. Data points are mean ± s.e.m. (n = 95-121).

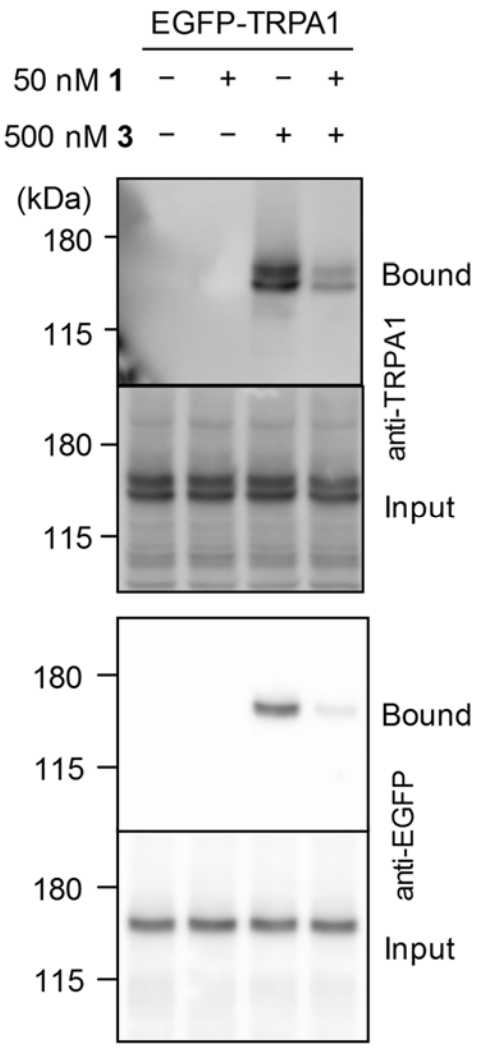

Figure S3. Detection of biotinylated EGFP-TRPA1 using anti-TRPA1 antibody. EGFP-TRPA1 transfected HEK293 cells were pre-treated with molecule 1 (50 nM) or DMSO for 10 min. Subsequently, the cells were incubated with molecule 3 (500 nM) or DMSO for 10 min. Unreacted molecules were washed out and the biotinylated proteins were purified from the cells by avidin beads. The purified samples (Bound) and the cell lysate (Input) were analyzed by western blotting with a TRPA1 antibody or an EGFP antibody.

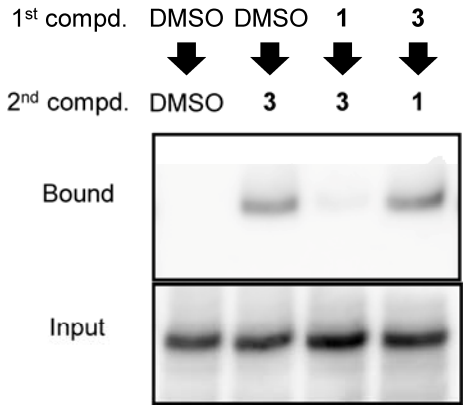

Figure S4. Subsequent treatment with molecule **1** had no detectable impacts on the biotinylation of TRPA1 by molecule **3**. EGFP-TRPA1 transfected HEK293 cells were pretreated with 1st compounds for 10 min. After extensive wash by PBS, the cells were incubated with 2nd compounds for 10 min. Unreacted molecules were washed out and the biotinylated proteins were purified from the cells by avidin beads. The purified samples (Bound) and the cell lysate (Input) were analyzed by western blotting with an EGFP antibody. 50 nM molecule **1**, 500 nM molecule **3**, or DMSO control were used.

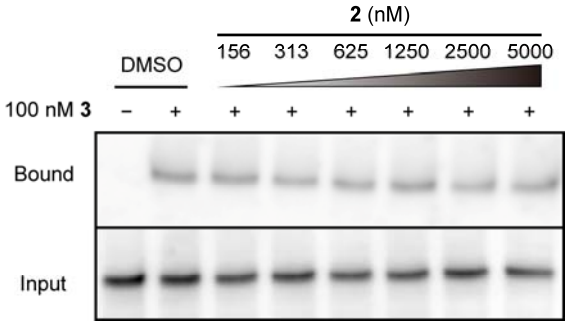

Figure S5. Pretreatments with molecule **2** had no impacts on the biotinylation of TRPA1 by molecule **3**. EGFP-TRPA1 transfected HEK293 cells were incubated with molecule **2** at the various concentrations or DMSO control for 10 min. The cells were subsequently incubated with 100 nM molecule **3**. After extensive wash, the cells were lysed and biotinylated proteins were purified from the centrifuged supernatants by avidin beads. The purified samples (Bound) and the supernatants (Input) were analyzed by western blot analysis with an EGFP antibody.

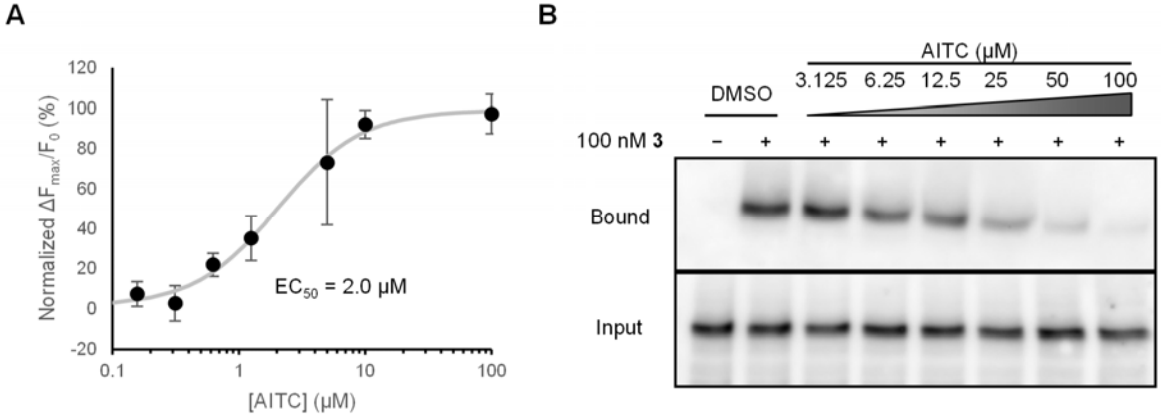

Figure S6. AITC prevents the biotinylation of TRPA1 by molecule **3** at high concentrations. (A) A dose-response curve for AITC-induced Fluo-8 fluorescence changes. Fluorescence changes were normalized to the response evoked by 100 μM AITC. The plots were fitted to a four parameter logistic model using an Image J software. The EC_{50} value was calculated to be 2 μM. The data points are mean ± s.e.m. (n = 5-6). (B) EGFP-TRPA1 transfected HEK293 cells were pretreated with AITC at the various concentrations for 10 min, and the cells were subsequently incubated with molecule **3** for 10 min. After extensive wash, the cells were lysed and biotinylated proteins were purified from the supernatants by avidin beads. The purified samples (Bound) and the supernatants (Input) were analyzed by western blot analysis with an EGFP antibody.

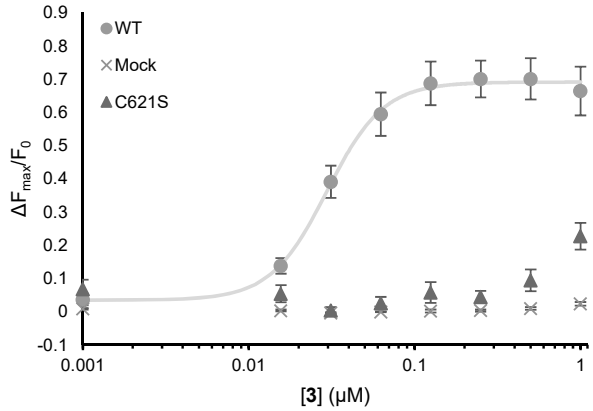

Figure S7. Dose-response curves for molecule **3**-induced Fluo-8 fluorescence changes in TRPA1 wild type (WT)-, C621S mutant- or mock-transfected HEK293 cells. The data points are mean ± s.e.m. (n = 6-20).

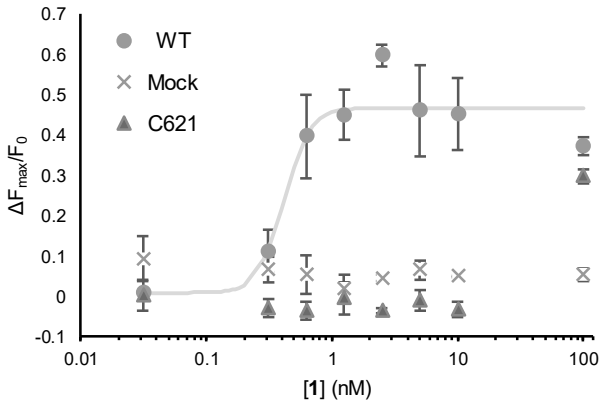

Figure S8. TRPA1 C621S mutant has a low sensitivity to molecule **1**. Dose-response curves for molecule **1**-induced Fluo-8 fluorescence changes in TRPA1 wild type (WT)-, C621S mutant- or mock-transfected HEK293 cells. The data points are mean ± s.e.m. (n = 3).

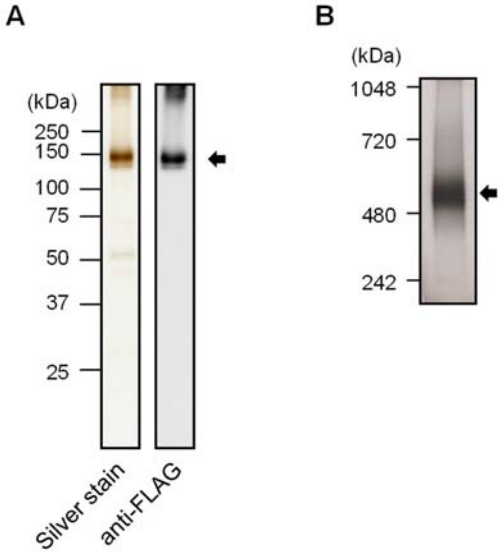

Figure S9. Analysis of purified FLAG-TRPA1. (A) Purified FLAG-TRPA1 was analyzed by silver staining or western blotting with an anti-FLAG antibody. FLAG-TRPA1 was purified with immunoaffinity chromatography followed by SEC. The purified FLAG-TRPA1 was detected at ~150 kDa, as indicated by an arrow. (B) Blue native PAGE analysis of the purified FLAG-TRPA1. The purified FLAG-TRPA1 was detected at ~560 kDa, as indicated by an arrow.

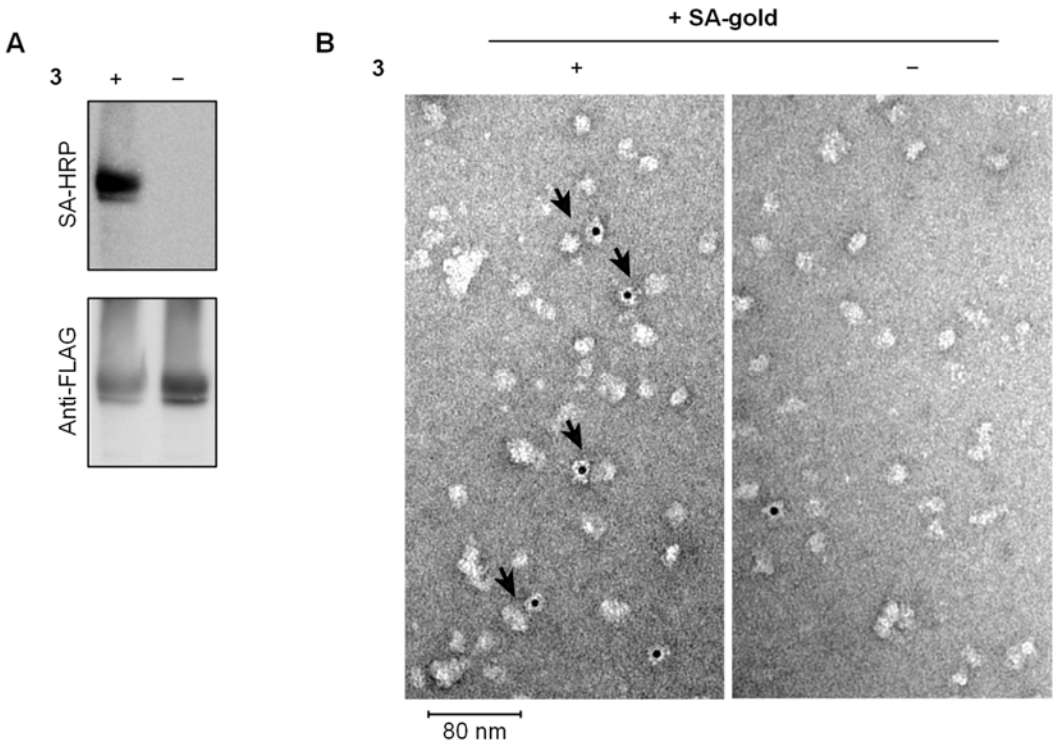

Figure S10. Visualization of negatively stained gold-nanoparticle-labeled molecule **3** and FLAG-TRPA1 by electron microscopy. (A) FLAG-TRPA1 was treated with molecule **3** (5 μM) for 1h. The sample was mixed with an anti-FLAG affinity gel (Sigma). Unreacted molecule **3** was washed out with a wash buffer (TBS containing 1 mM DDM, 300 mM $MgCl_2$, 0.02% sodium azide). Molecule **3**-treated FLAG-TRPA1 was eluted with a wash buffer containing FLAG peptide. Eluate was analyzed by affinity/western blotting with streptavidin-HPR (SA-HRP) or FLAG antibodies. (B) FLAG-TRPA1 was treated with/without molecule **3** under the same conditions as A. After extensive wash, streptavidin-gold conjugate (SA-gold) was added to the sample. Unbound SA-gold was removed with the wash buffer, and FLAG-TRPA1 was eluted with a wash buffer containing a FLAG peptide. Eluates were visualized by electron microscopy with negative staining.

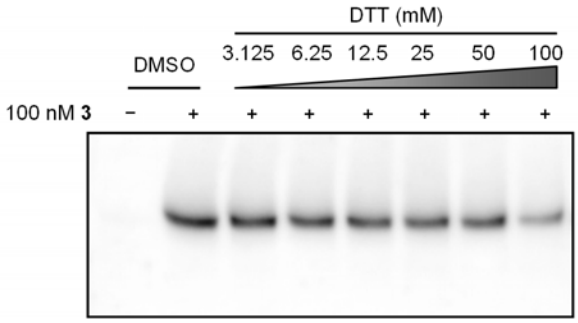

Figure S11. Limited effects of DTT on the ability of molecule **3** to bind EGFP-TRPA1. EGFP-TRPA1 transfected HEK293 cells were incubated with molecule **3** (100 nM) for 10 min in the presence of DTT at the various concentrations. After extensive wash, the cells were lysed, and the biotinylated proteins were purified by avidin beads. The samples were analyzed by western blot analysis with an anti-EGFP antibody.

Chemical synthesis

General. Unless otherwise noted all solvents and chemicals for chemical synthesis were purchased used without further purification. 2-Bromo-4'-methoxyacetophenone was purchased from Sigma-Aldrich Co. LLC. (St. Louis, MO, USA). Thiourea, 3-methoxypropionic acid, lithium aluminium hydride, chloroacetyl chloride, acetic anhydride, 1,6-dibromohexane and boron tribromide (1.0 M in dicloromethane) were purchased from Wako Pure Chemical Industries Ltd. (Osaka, Japan). *O*-(6-Chloro-1*H*-benzotriazol-1-yl)-*N*,*N*,*N*',*N*'-tetramethyluronium hexafluorophosphate (HCTU) and di-*tert*-butyl dicarbonate (Boc_2O) were purchased from Watanabe Chemical Industries, Ltd. (Hiroshima, Japan). Biotin-NHS were purchased from Molecular Biosciences, Inc. (Colorado, USA). Amino-functionalized silica gel NH-DM1020 was purchased from Fuji Silysia chemical Ltd. (Aichi, Japan). All other solvents and chemicals for chemical synthesis were purchased from Tokyo Chemical Industry Co., Ltd. (Tokyo, Japan) or Nacalai Tesque, Inc. (Kyoto, Japan). Some synthetic compounds were purified using a flash column system Shoko Scientific Purif-α2. High performance liquid chromatography (HPLC) was performed with combined system of Shimadzu DGU-20A_3 (degasser), LC-20AD (pump ×2), CTO-20AC (column oven), SPD-20A (detector) and CBM-20Alite (controller). HPLC conditions were as follows: Shimadzu Shim-pack XR-ODS column (2.2 μm, 3.0 × 50 mm); solvent gradient, A, 0.1% trifluoroacetic acid (TFA) in H_2O; B, acetonitrile with gradient (0–3.5 min: B, 10–100%; 3.5–5 min: B, 100% at 40 °C); flow rate, 0.7 mL/min; detector, 254 nm. Low-resolution mass spectra were obtained using a Shimadzu LCMS-2010EV in ESI mode. High-resolution mass spectra (HRMS) were obtained using a JEOL MStation JMS-700 in FAB mode. Solution ^{1}H-NMR spectra were collected by JEOL JNM-ECP 300 MHz. Chemical shifts were reported in δ (ppm) relative to tetramethylsilane.

Scheme S1. Chemical synthesis of 1 and 2

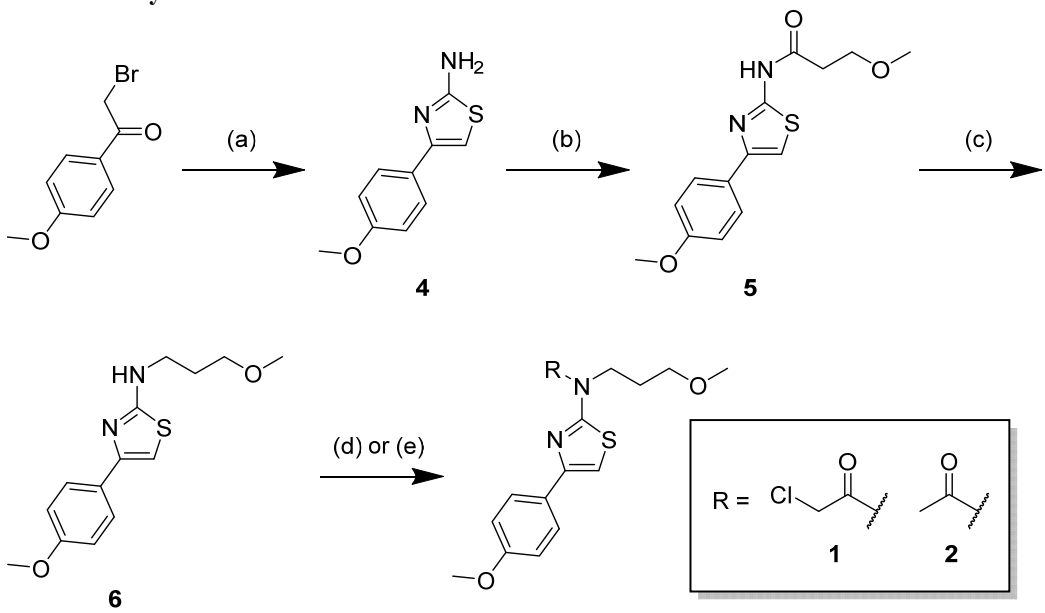

Conditions and reagents: (a) thiourea, EtOH, reflux, 2 h, quant. (b) 3-methoxypropanoic acid, DIPEA, HCTU, DMF, rt, 96 h, 59% (c) $LiAlH_4$, THF, 0 °C, 6 h, 97% (d) chloroacetyl chloride, TEA, AcOEt, 0 °C, 4 h, 43% (e) acetic anhydride, pyridine, rt, 18 h, 75%

4-(4-Methoxyphenyl)thiazol-2-amine (4)

To a solution of 2-bromo-4'-methoxyacetophenone (2.5 g, 10.9 mmol) in ethanol (EtOH) (20 mL) was added thiourea (0.86 g, 11.3 mmol) and the mixture was refluxed for 2 h. After the solvent was removed, the resulting white precipitate was suspended and washed in water/saturated aqueous $NaHCO_3$ (30/70, 10 mL) for 1 h. The precipitate was collected by filtration, and azeotroped with toluene *in vacuo* to give **4** (2.55 g, 10.9 mmol, quant.) as a white powder, which was used without further purification. ^{1}H-NMR (300 MHz, DMSO-d_6): δ 8.11 (2H, br s), 7.68 (2H, d, J = 9.1 Hz), 7.01 (2H, d, J = 9.1 Hz), 6.98 (1H, s), 3.79 (3H, s); ESI-MS m/z: 207 $[M+H]^+$.

3-Methoxy-*N*-(4-(4-methoxyphenyl)thiazol-2-yl)propanamide (5)

To a solution of **4** (1.76 g, 8.53 mmol), 3-methoxypropionic acid (1.23 mL, 12.8 mmol) and *N*,*N*-diisopropylethylamine (DIPEA) (2.23 mL, 12.8 mmol) in *N*,*N*-dimethylformamide (DMF) (30 mL) was added HCTU (5.29 g, 12.8 mmol) and the mixture was stirred at room temperature for 96 h. The reaction mixture was diluted with ethyl acetate (AcOEt) and washed with saturated aqueous $NaHCO_3$, hydrochloric acid (0.5 M), water and brine. The organic layer was dried over Na_2SO_4 and concentrated *in vacuo*. The resulting precipitate was suspended and washed in AcOEt/hexane (50/50, 50 mL) for 1 h. The precipitate was collected by filtration to give **5** (1.46 g, 5.00 mmol, 59%) as a white powder, which was used without further purification. ^{1}H-NMR (300 MHz, DMSO-d_6): δ 12.23 (1H, s), 7.82 (2H, d, J = 8.6 Hz), 7.44 (1H, s), 6.99 (2H, d, J = 8.6 Hz), 3.79 (3H, s), 3.64 (2H, t, J = 6.0 Hz), 3.24 (3H, s), 2.69 (2H, t, J = 6.0 Hz); ESI-MS m/z: 293 $[M+H]^+$.

4-(4-Methoxyphenyl)-*N*-(3-methoxypropyl)thiazol-2-amine (6)

To a suspension of lithium aluminium hydride (350 mg, 9.22 mmol) in anhydrous tetrahydrofuran (THF) (5 mL) was added a solution of **5** (703 mg, 2.40 mmol) in anhydrous THF (5 mL) dropwise over 30 min and the mixture was stirred at 0 °C for 6 h under an argon atmosphere. To the reaction mixture were added water (0.35 mL), aqueous NaOH (15%w/v, 0.35 mL) and extra water (1.05 mL) in order. The resulting mixture was filtered through a pad of celite with AcOEt. The filtrate was washed with saturated aqueous $NaHCO_3$ twice, saturated aqueous NH_4Cl and brine. The organic layer was dried over Na_2SO_4 and concentrated *in vacuo* to give **6** (650 mg, 2.34 mmol, 97%) as a yellow oil, which was used without further purification. ^{1}H-NMR (300 MHz, $CDCl_3$): δ 7.73 (2H, d, *J* = 8.8 Hz), 6.90 (2H, d, *J* = 8.8 Hz), 6.55 (1H, s), 5.57-5.48 (1H, m), 3.83 (3H, s), 3.53 (2H, t, *J* = 5.7 Hz), 3.41 (2H, m), 3.36 (3H, s), 1.94 (2H, m); ESI-MS *m*/*z*: 279 $[M+H]^+$.

2-Chloro-*N*-(4-(4-methoxyphenyl)thiazol-2-yl)-*N*-(3-methoxypropyl)acetamide (1)

To a solution of **6** (227 mg, 0.815 mmol) and triethylamine (TEA) (115 µL, 0.818 mmol) in AcOEt (5 mL) was added chloroacetyl chloride (168.3 µL, 1.06 mmol) dropwise over 30 min at 0 °C and the mixture was stirred at 0 °C for 4 h. The reaction mixture was diluted with AcOEt and washed with saturated aqueous $NaHCO_3$, saturated aqueous NH_4Cl and brine. The organic layer was concentrated *in vacuo*, and the resulting residue was purified by silica gel column chromatography to give **1** (124.44 mg, 0.351 mmol, 43%) as a pale yellow crystal. ^{1}H-NMR (300 MHz, $CDCl_3$): δ 7.81 (2H, d, *J* = 8.6 Hz), 7.10 (1H, s), 6.95 (2H, d, *J* = 8.6 Hz), 4.53 (2H, s), 4.45-4.29 (2H, m), 3.85 (3H, s), 3.44 (2H, t, *J* = 5.5 Hz), 3.36 (3H, s), 2.26-2.12 (2H, m); ESI-MS *m*/*z*: 355 $[M+H]^+$; FAB-MS calcd for $C_{16}H_{19}ClN_2O_3S$ $[M^+]$: 354.0805; found: 354.0804.

***N*-(4-(4-Methoxyphenyl)thiazol-2-yl)-*N*-(3-methoxypropyl)acetamide (2)**

To a solution of **6** (80 mg, 0.28 mmol) in pyridine (2 mL) was added acetic anhydride (32 µL, 0.34 mmol) and the mixture was stirred at room temperature for 18 h. The reaction mixture was diluted with AcOEt and washed with saturated aqueous $NaHCO_3$ and brine. The organic layer was dried over Na_2SO_4 and concentrated *in vacuo*. The resulting residue was purified by amino-functionalized silica gel column chromatography (10% AcOEt in hexane) to give **2** (67.2 mg, 0.210 mmol, 75%) as a white powder. ^{1}H-NMR (300 MHz, $CDCl_3$): δ 7.82 (2H, d, *J* = 8.4 Hz), 7.04 (1H, s), 6.94 (2H, d, *J* = 8.4 Hz), 4.36 (2H, t, *J* = 6.6 Hz), 3.85 (3H, s), 3.48 (2H, t, *J* = 5.7 Hz), 3.36 (3H, s), 2.46 (3H, s), 2.15 (2H, m); ESI-MS *m*/*z*: 321 $[M+H]^+$; FAB-MS calcd for $C_{16}H_{20}N_2O_3S$ $[M^+]$: 320.1195; found: 320.1196.

Scheme S2. Chemical synthesis of 3

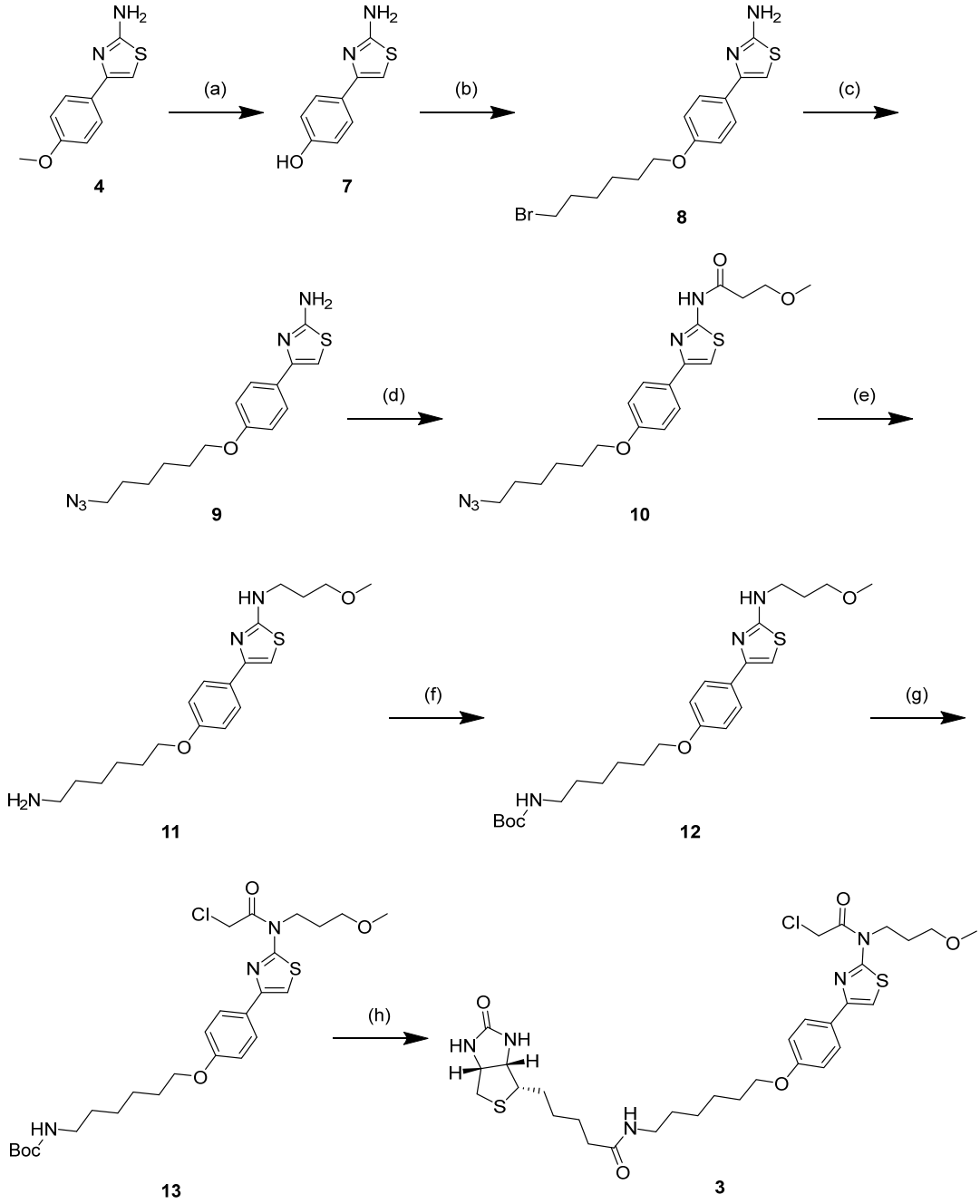

Conditions and reagents: (a) BBr_3, CH_2Cl_2, 0 °C-rt, 48 h, 61% (b) 1,6-dibromohexane, K_2CO_3, acetone, reflux, 20 h, 65% (c) NaN_3, DMSO, rt, 12 h, 34% (d) 3-methoxypropionic acid, HCTU, DIPEA, DMF, rt, 14 h, 87% (e) $LiAlH_4$, THF, 0 °C, 2 h, 83% (f) Boc_2O, MeOH, rt, 1 h, 73% (g) Chloroacetyl chloride, TEA, AcOEt, 0 °C, 6 h, 40% (h) (i) TFA, $CHCl_3$, rt, 30 min; (ii) Biotin-NHS, TEA, DMSO, rt, 30 min, 72%

4-(2-Aminothiazol-4-yl)phenol (7)

To a solution of **4** (4.5 g, 21.8 mmol) in dichloromethane (116 mL) was added a solution of boron tribromide in dichloromethane (1.0 M, 64 mL) dropwise over 30 min at 0 °C and the mixture was stirred at room temperature for 48 h under an argon atmosphere. After dilution with AcOEt, the resulting mixture was neutralized with saturated aqueous $NaHCO_3$ and washed with brine. The organic layer was dried over Na_2SO_4 and concentrated *in vacuo*. The resulting precipitate was collected by filtration to give **7** (2.57 g, 13.4 mmol, 61%) as a brown powder, which was used without further purification. ^{1}H-NMR (300 MHz, DMSO-d_6): δ 9.44 (1H, s), 7.59 (2H, d, J = 8.8 Hz), 6.95 (2H, s), 6.76-6.70 (3H, m).

4-(4-((6-Bromohexyl)oxy)phenyl)thiazol-2-amine (8)

To a mixture of **7** (2.57 g, 13.4 mmol) and potassium carbonate (2 g, 14.5 mmol) in acetone (200 mL) was added 1,6-

dibromohexane (4.29 mL, 28.2 mmol) and the mixture was refluxed for 20 h. The reaction mixture was diluted with water and the aqueous layer was extracted with AcOEt four times. The combined organic layers were washed with brine, dried over Na_2SO_4 and concentrated *in vacuo*. The resulting residue was purified by silica gel column chromatography (33% AcOEt in hexane) to give **8** (3.1 g, 8.73 mmol, 65%) as a white powder. ^{1}H-NMR (300 MHz, DMSO-d_6): δ 7.70 (2H, d, *J* = 8.8 Hz), 6.98 (2H, s), 6.90 (2H, d, *J* = 8.8 Hz), 6.81 (1H, s), 3.97 (2H, t, *J* = 6.3 Hz), 3.54 (2H, t, *J* = 6.6 Hz), 1.88-1.77 (2H, m), 1.76-1.67 (2H, m) 1.49-1.40 (4H, m).

4-(4-((6-Azidohexyl)oxy)phenyl)thiazol-2-amine (9)

To a mixture of **8** (3.1 g, 8.7 mmol) in DMSO (80 mL) was added sodium azide (851 mg, 13.1 mmol) and the mixture was stirred at room temperature for 12 h under an argon atmosphere. The reaction mixture was diluted with water and the aqueous layer was extracted with ether twice. The combined organic layers were washed with water, brine, dried over Na_2SO_4 and concentrated *in vacuo*. The resulting precipitate was collected by filtration to give **9** (951.2 mg, 3.0 mmol, 34%), which was used without further purification. ^{1}H-NMR (300 MHz, DMSO-d_6): δ 7.70 (2H, d, *J* = 8.8 Hz), 6.98 (2H, s), 6.90 (2H, d, *J* = 8.8 Hz), 6.81 (1H, s), 3.97 (2H, t, *J* = 6.5 Hz), 3.33 (2H, t, *J* = 6.9 Hz), 1.77-1.66 (2H, m), 1.62-1.51 (2H, m), 1.50-1.33 (4H, m); ESI-MS m/z: 318 $[M+H]^+$.

***N*-(4-(4-((6-Azidohexyl)oxy)phenyl)thiazol-2-yl)-3-methoxypropanamide (10)**

To a mixture of **9** (900 mg, 2.84 mmol), 3-methoxypropionic acid (408 µL, 4.3 mmol) and DIPEA (750 µL, 4.3 mmol) in DMF (10 mL) was added HCTU (1.76 g, 4.3 mmol) and the mixture was stirred at room temperature for 14 h. The reaction mixture was diluted with AcOEt and washed with saturated aqueous $NaHCO_3$, water and brine. The organic layer was dried over Na_2SO_4 and concentrated *in vacuo*. The resulting precipitate was collected to give **10** (1.00 g, 2.47 mmol, 87%), which was used without further purification. ^{1}H-NMR (300 MHz, DMSO-d_6): δ 12.22 (1H, s), 7.80 (2H, d, *J* = 8.8 Hz), 7.43 (1H, s), 6.97 (2H, d, *J* = 8.8 Hz), 3.99 (2H, t, *J* = 6.5 Hz), 3.64 (2H, t, *J* = 6.1 Hz), 3.37-3.30 (2H, m), 3.24 (3H, s), 2.69 (2H, t, *J* = 6.2 Hz), 1.79-1.66 (2H, m), 1.62-1.51 (2H, m), 1.50-1.34 (4H, m); ESI-MS m/z: 404 $[M+H]^+$.

4-(4-((6-Aminohexyl)oxy)phenyl)-*N*-(3-methoxypropyl)thiazol-2-amine (11)

To a suspension of lithium aluminium hydride (468.8 mg, 12.4 mmol) in anhydrous THF (5 mL) was added a solution of **10** (1 g, 2.47 mmol) in anhydrous THF (5 mL) dropwise over 30 min and the mixture was stirred at 0 °C for 1 h under an argon atmosphere. To the reaction mixture were added water (0.47 mL), aqueous NaOH (15%w/v, 0.47 mL) and extra water (1.4 mL) in order. The resulting mixture was filtered through a pad of celite with AcOEt. The filtrate was washed with saturated aqueous $NaHCO_3$ twice, saturated aqueous NH_4Cl and brine. The organic layer was dried over Na_2SO_4 and concentrated *in vacuo* to give **11** (740.6, 2.04 mmol, 83%), which was used without further purification. ^{1}H-NMR (300 MHz, DMSO-d_6): δ 7.72 (2H, d, *J* = 8.8 Hz), 7.63-7.54 (1H, m), 6.91 (2H, d, *J* = 8.8 Hz), 6.85 (1H, s), 3.96 (2H, t, *J* = 6.5 Hz), 3.41 (2H, t, *J* = 6.3 Hz), 3.33-3.25 (2H, m), 3.24 (3H, s), 3.20-2.80 (2H, br s), 2.57-2.50 (2H, m), 1.87-1.76 (2H, m), 1.76-1.65 (2H, m), 1.47-1.30 (6H, m); ESI-MS m/z: 364 $[M+H]^+$.

***tert*-Butyl (6-(4-(2-((3-methoxypropyl)amino)thiazol-4-yl)phenoxy)hexyl)carbamate (12)**

To a solution of **11** (717 mg, 1.97 mmol) in methanol (MeOH) (1.5 mL) was added Boc_2O (480 mg, 2.2 mmol) in MeOH (0.6 mL) dropwise and the mixture was stirred at room temperature for 1 h. The reaction mixture was concentrated *in vacuo* and the resulting residue was purified by silica gel column chromatography to give **12** (669.6 mg, 1.44 mmol, 73%) as a yellow oil. ^{1}H-NMR (300 MHz, $CDCl_3$): δ 7.71 (2H, d, *J* = 8.8 Hz), 6.88 (2H, d, *J* = 8.8 Hz), 6.54 (1H, s), 5.78 (1H, br s), 4.51 (1H, br s), 3.96 (2H, t, *J* = 6.6 Hz), 3.53 (2H, t, *J* = 5.8 Hz), 3.44-3.38 (2H, m), 3.36 (3H, s), 3.17-3.06 (2H, m), 1.99-1.89 (2H, m), 1.84-1.73 (2H, m), 1.56-1.32 (15H, m); ESI-MS m/z: 464 $[M+H]^+$.

***tert*-Butyl (6-(4-(2-(2-chloro-*N*-(3-methoxypropyl)acetamido)thiazol-4-yl)phenoxy)hexyl)carbamate (13)**

To a solution of **12** (95.4 mg, 0.206 mmol) and TEA (34.7 µL, 0.247 mmol) was added chloroacetyl chloride (17.8 µL, 0.222 mmol) dropwise and stirred at 0 °C for 6 h. The reaction mixture was diluted with AcOEt and washed with saturated aqueous $NaHCO_3$ and brine. The organic layer was dried over Na_2SO_4 and concentrated *in vacuo*. The resulting residue was purified by silica gel column chromatography (20% AcOEt in hexane) to give **13** (44.6 mg, 0.0826 mmol, 40%) as a yellow oil. ^{1}H-NMR (300 MHz, $CDCl_3$): δ 7.79 (2H, d, *J* = 8.9 Hz), 7.09 (1H, s), 6.92 (2H, d, *J* = 8.9 Hz), 4.57-4.46 (3H, m), 4.45-4.32 (2H, m), 3.99 (2H, t, *J* = 6.5 Hz), 3.44 (2H, t, *J* = 5.5 Hz), 3.36 (3H, s), 3.18-3.07 (2H, m), 2.25-2.14 (2H, m), 1.86-1.75 (2H, m), 1.58-1.38 (15H, m).

***N*-(6-(4-(2-(2-Chloro-*N*-(3-methoxypropyl)acetamido)thiazol-4-yl)phenoxy)hexyl)-5-((3a*S*,4*S*,6a*R*)-2-oxohexahydro-1*H*-thieno[3,4-*d*]imidazol-4-yl)pentanamide (3)**

To a solution of **13** (15.0 mg, 27.8 µmol) in chloroform (750 µL) was added TFA (250 µL) and the mixture was stirred at room temperature for 30 min. The reaction mixture was concentrated *in vacuo*. To a solution of the resulting oil in DMSO

(500 µL) were added a solution of biotin-NHS (17.4 mg, 51 µmol) and TEA (19.1 µL, 136 µmol) in DMSO (500 µL) and the mixture was stirred at room temperature for 30 min. The reaction mixture was lyophilized and the resulting residue was purified by PTLC (12.5% MeOH in $CHCl_3$) to give **3** (13.3 mg, 20.0 µmol, 72%) as a white solid. ^{1}H-NMR (300 MHz, DMSO-d_6): δ 7.85 (2H, d, J = 7.4 Hz), 7.76 (1H, t, J = 5.1 Hz), 7.58 (1H, s), 6.99 (2H, d, J = 7.4 Hz), 6.43 (1H, s), 6.36 (1H, s), 4.87 (2H, s), 4.33-4.20 (3H, m), 4.17-4.08 (1H, m), 3.99 (2H, t, J =6.3 Hz), 3.44 (2H, t, J = 5.8 Hz), 3.27 (3H, s), 3.13-2.98 (3H, m), 2.81 (1H, dd, J = 12.5, 4.7 Hz), 2.57 (1H, d, J = 12.5 Hz), 2.12-2.00 (4H, m), 1.77-1.67 (2H, m), 1.54-1.22 (12H, m); ESI-MS m/z: 666 $[M+H]^+$; FAB-MS calcd for $[C_{31}H_{44}ClN_5O_5S_2 + H]^+$: 666.2551; found: 666.2552.

^{1}H-NMR spectrum of **1** in $CDCl_3$

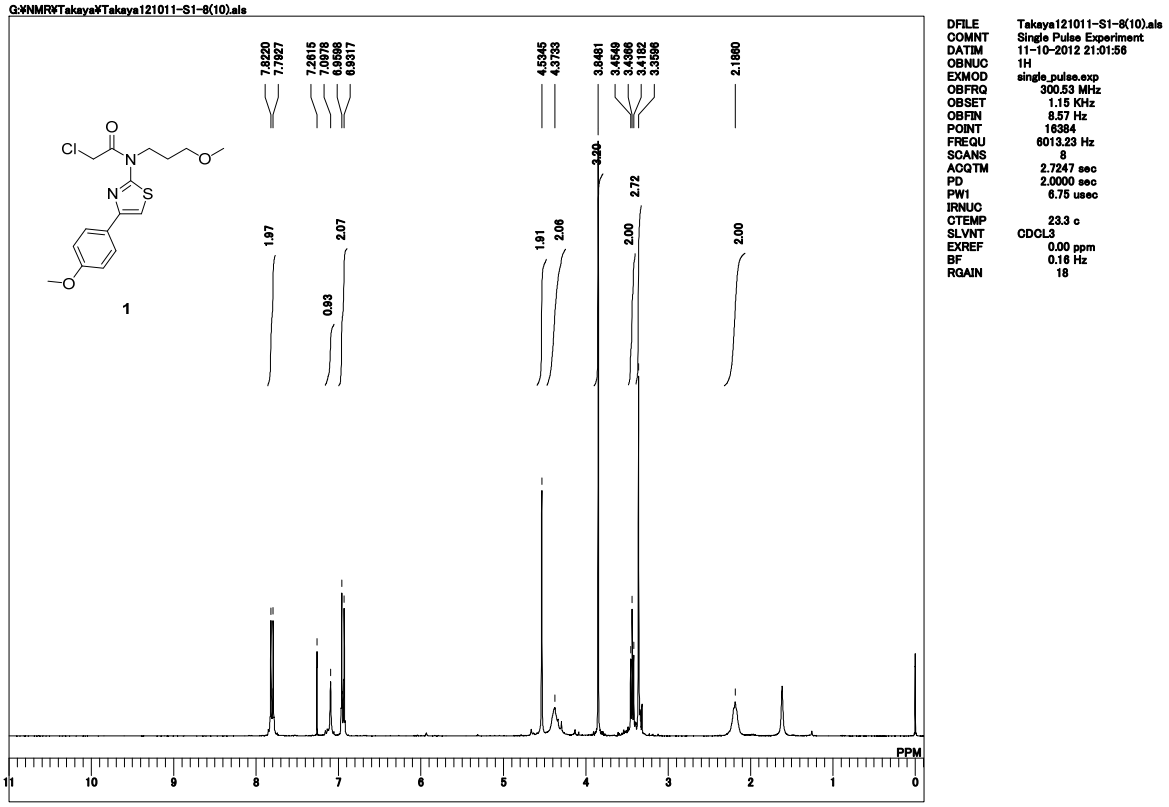

^{1}H-NMR spectrum of **2** in $CDCl_3$.

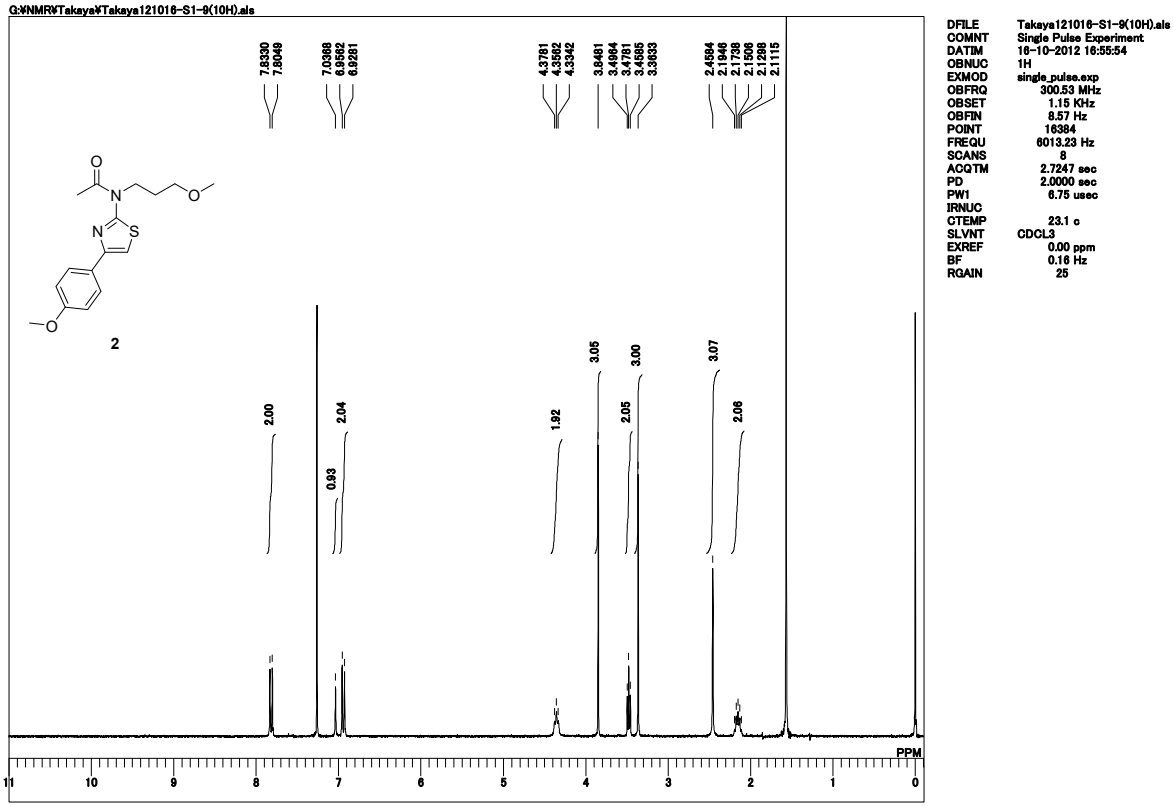

^{1}H-NMR spectrum of **3** in DMSO-d_6.

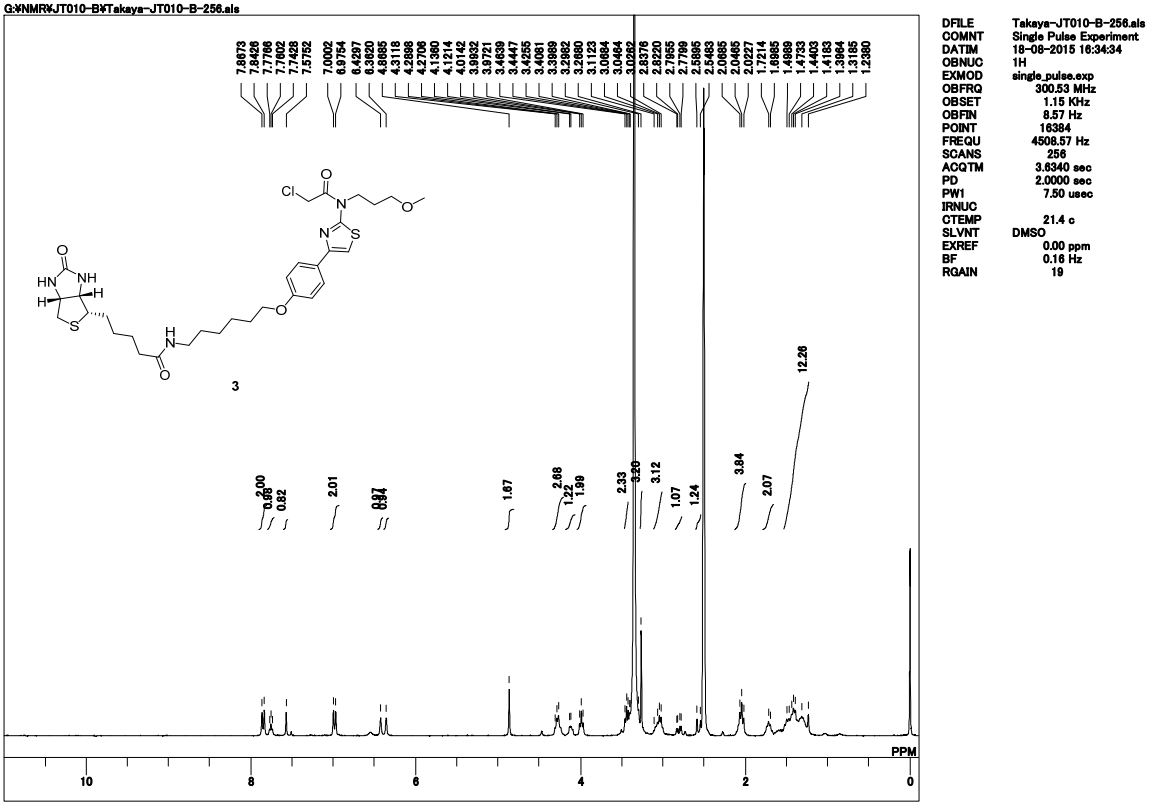

^{1}H-NMR spectrum of **4** in DMSO-d_6

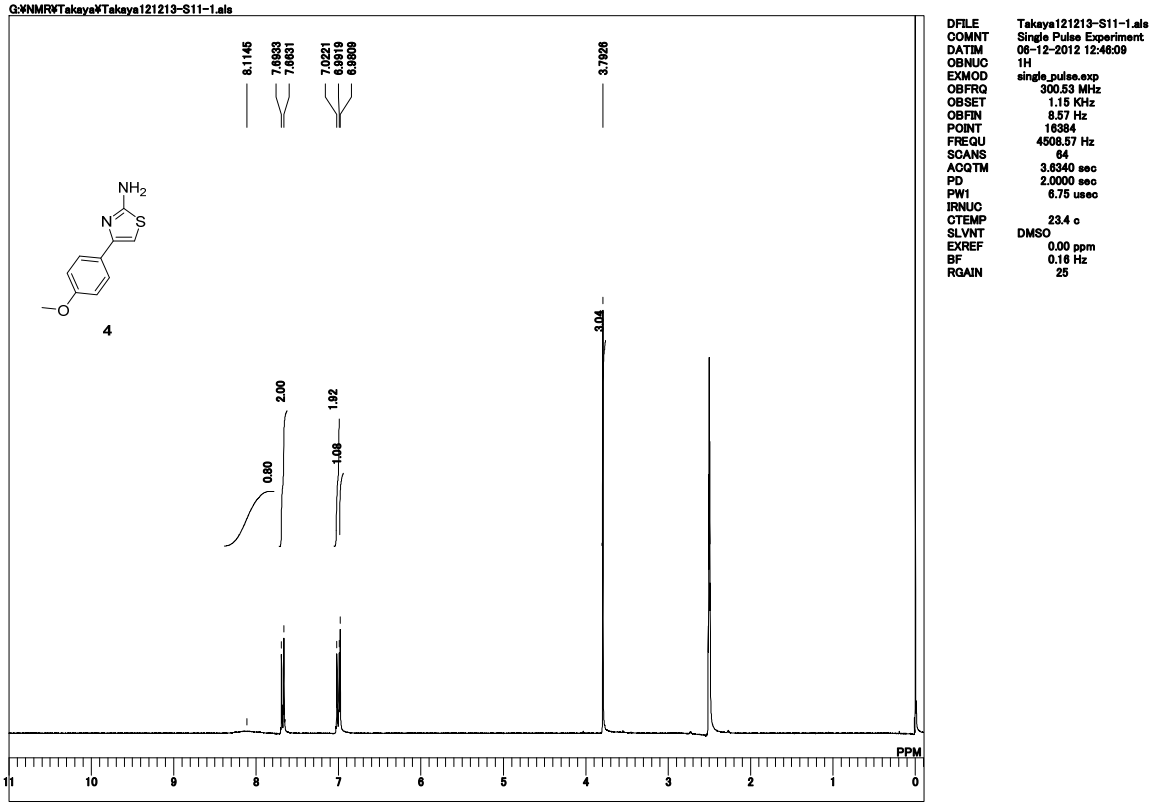

^{1}H-NMR spectrum of **5** in DMSO-d_6

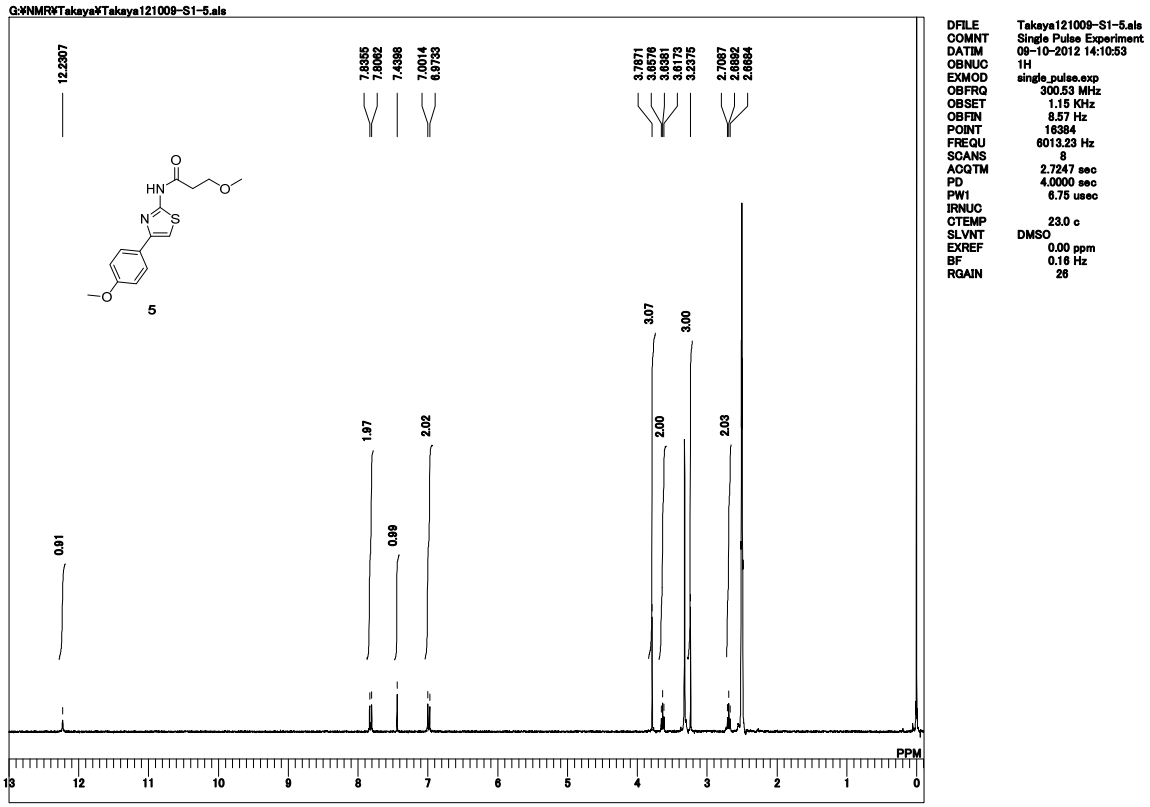

^{1}H-NMR spectrum of **6** in $CDCl_3$

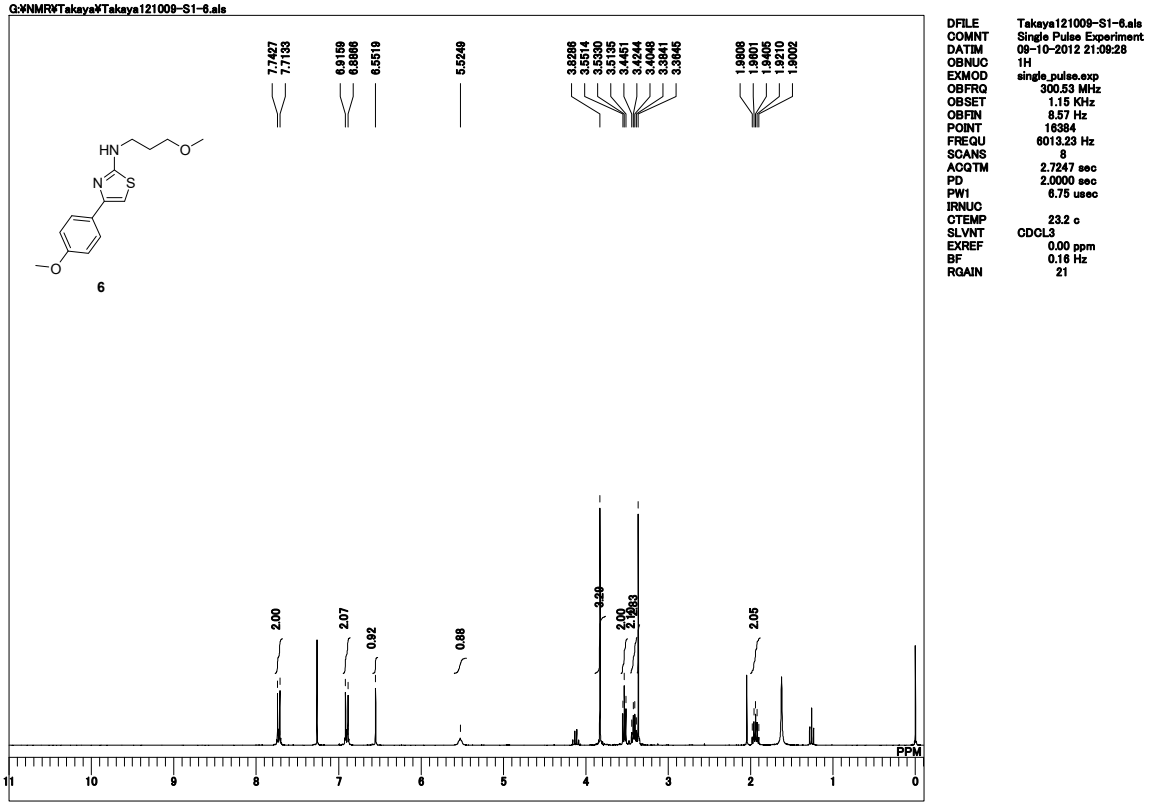

^{1}H-NMR spectrum of **7** in DMSO-d_6

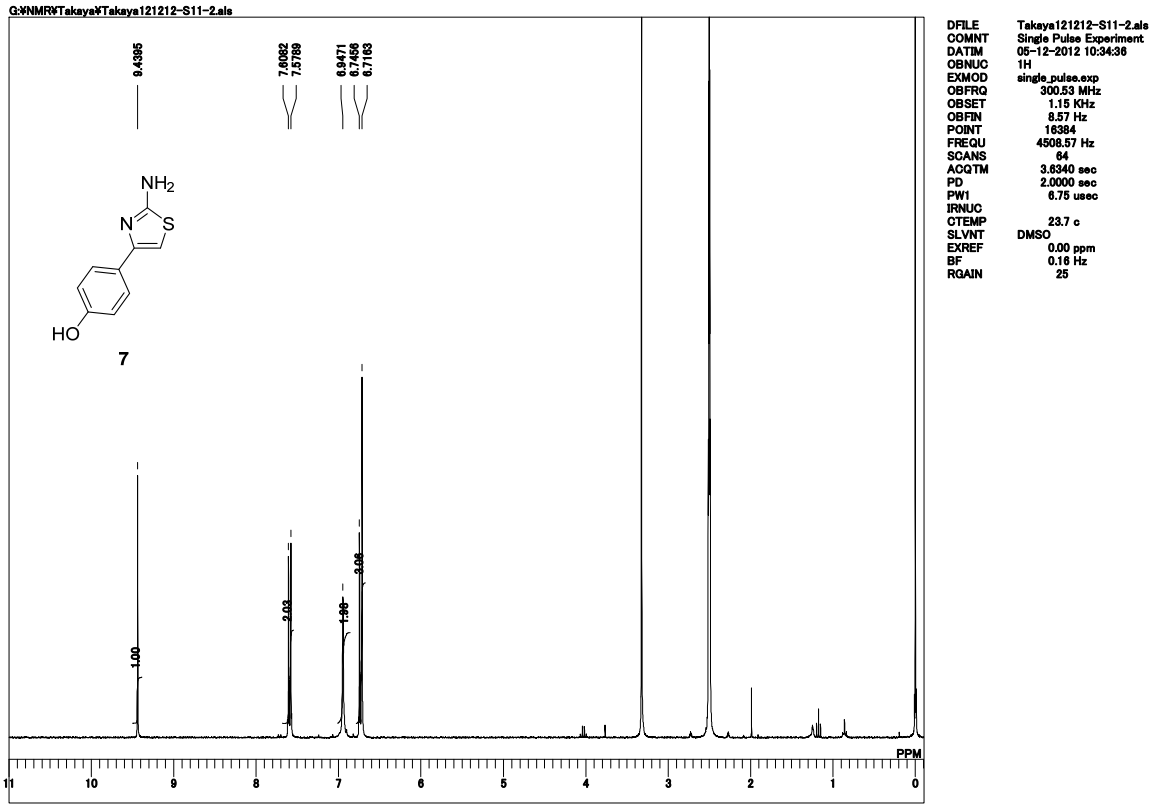

^{1}H-NMR spectrum of **8** in DMSO-d_6

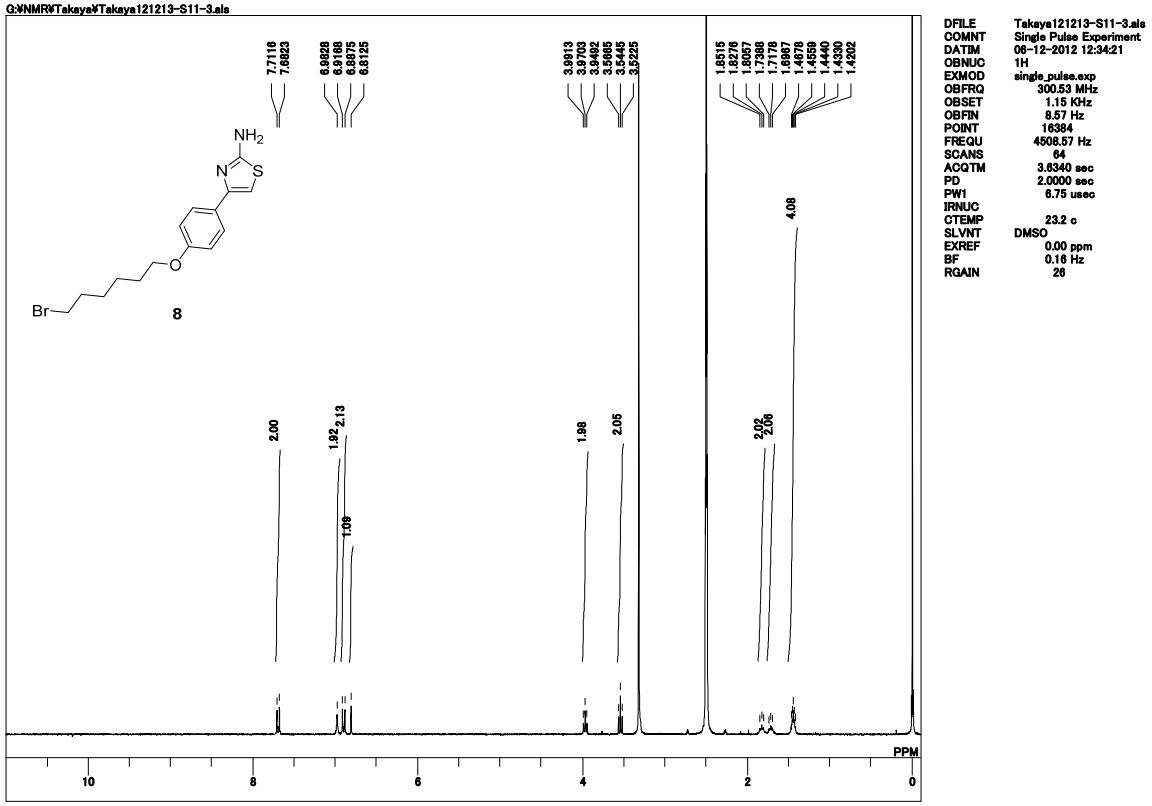

^{1}H-NMR spectrum of **9** in DMSO-d_6

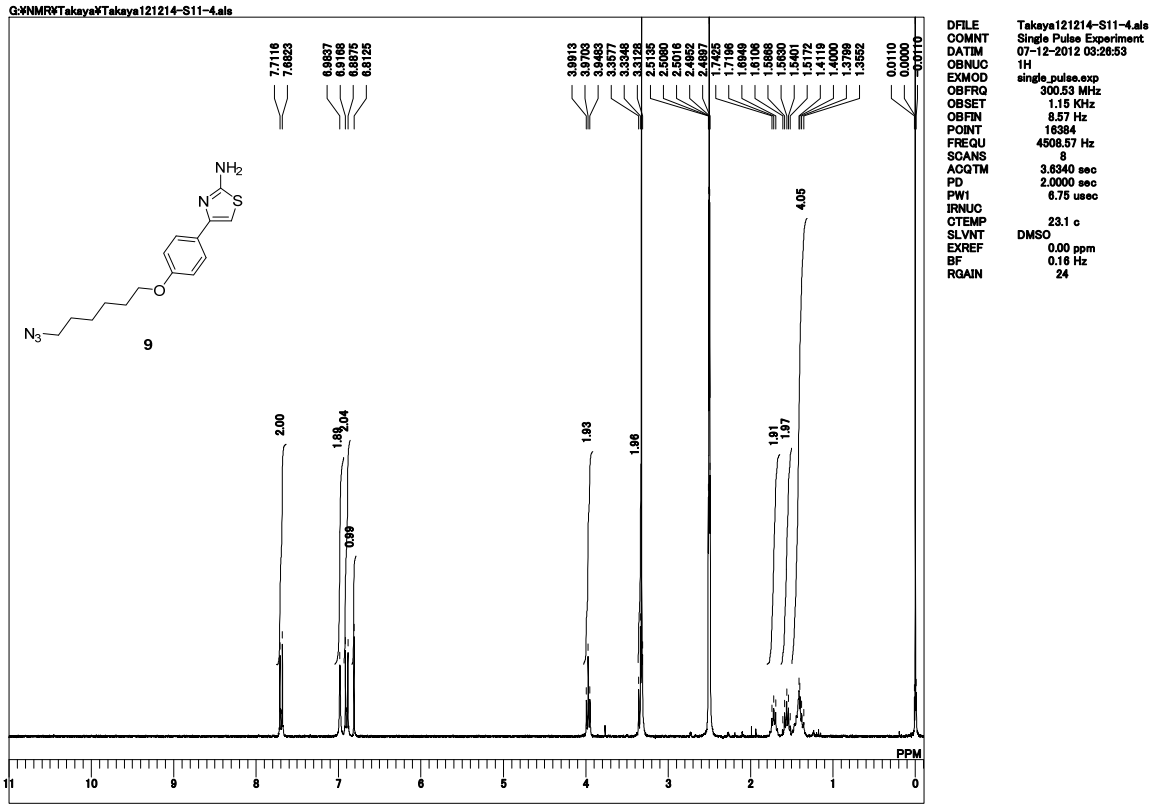

^{1}H-NMR spectrum of **10** in DMSO-d_6

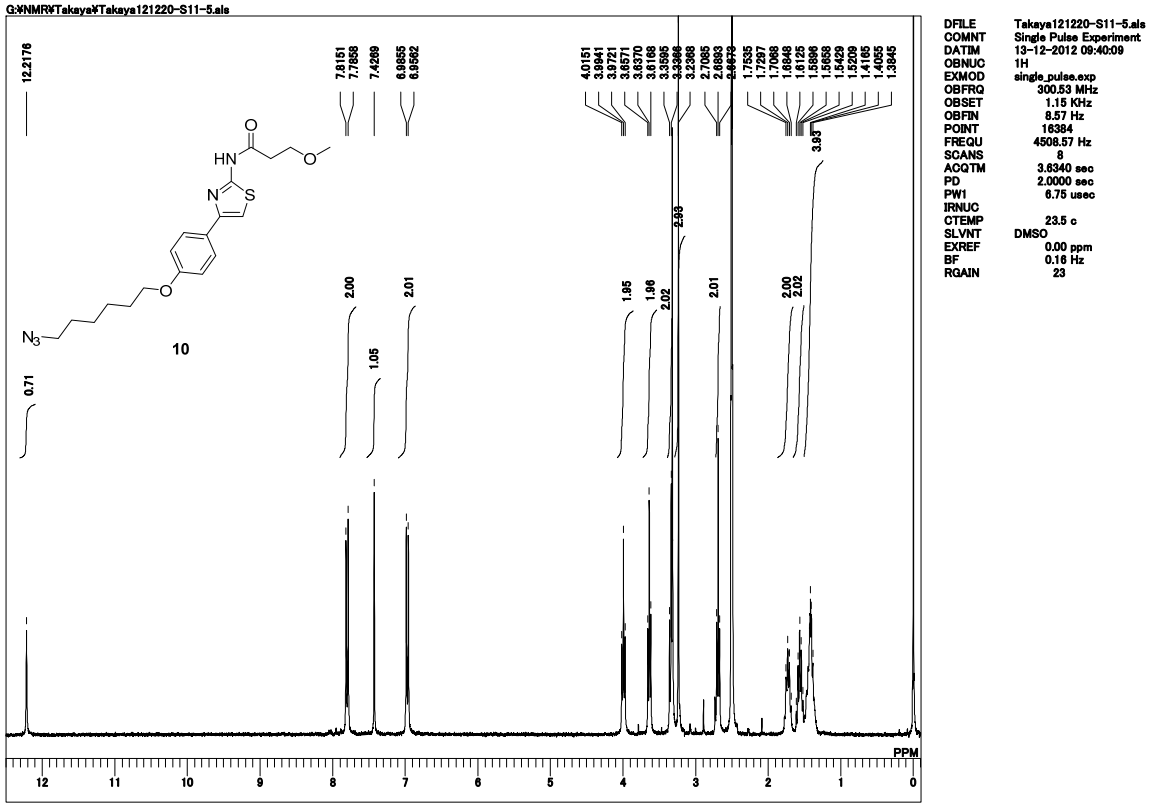

^{1}H-NMR spectrum of **11** in DMSO-d_6

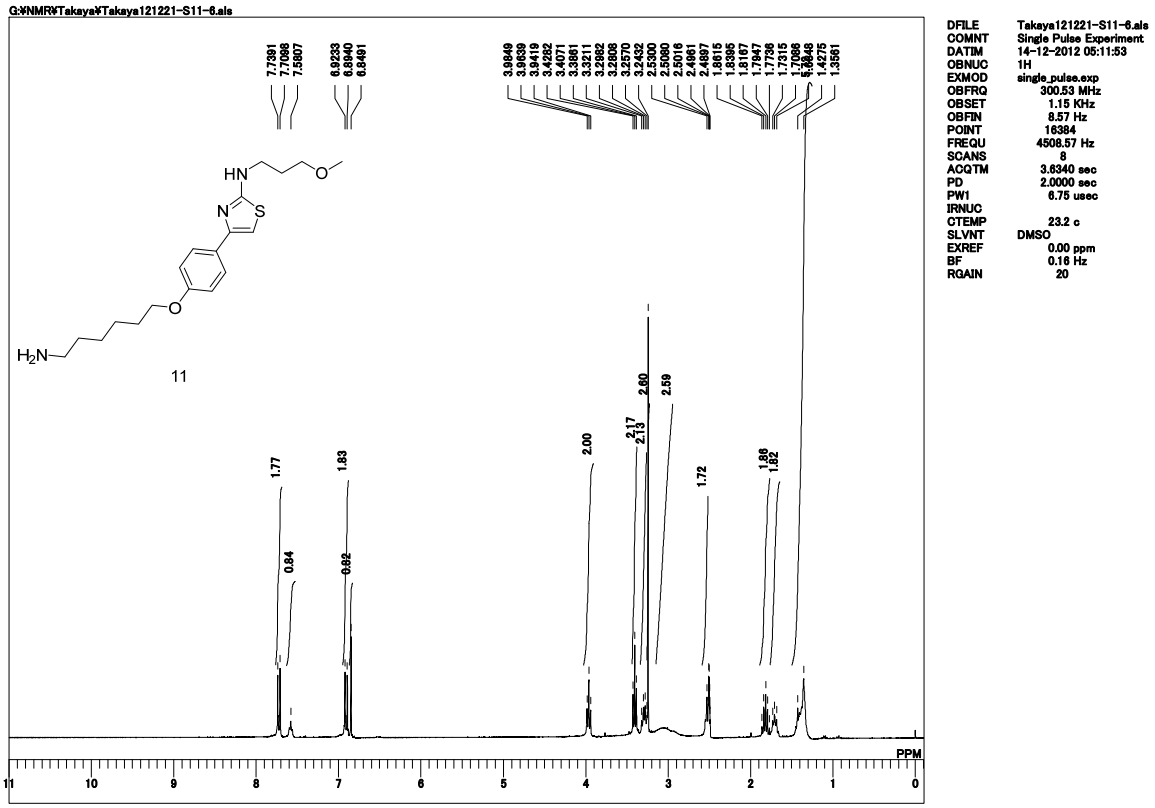

^{1}H-NMR spectrum of **12** in $CDCl_3$

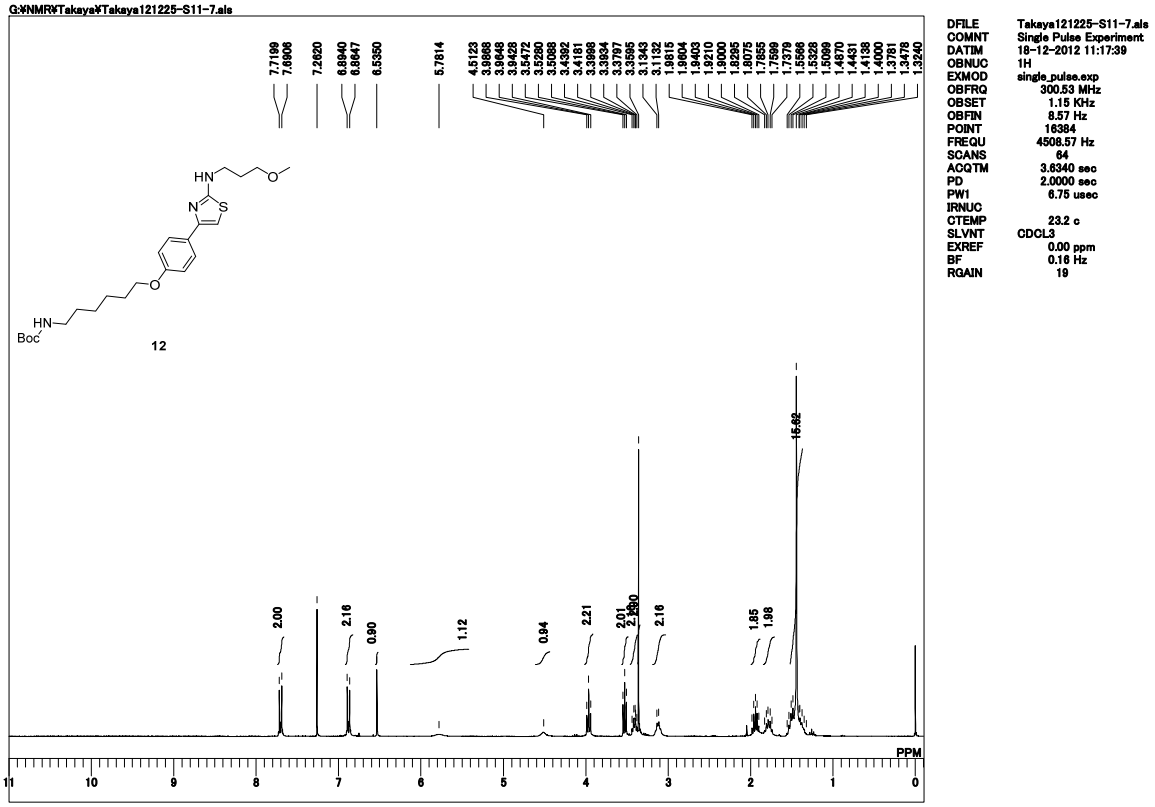

^{1}H-NMR spectrum of **13** in $CDCl_3$

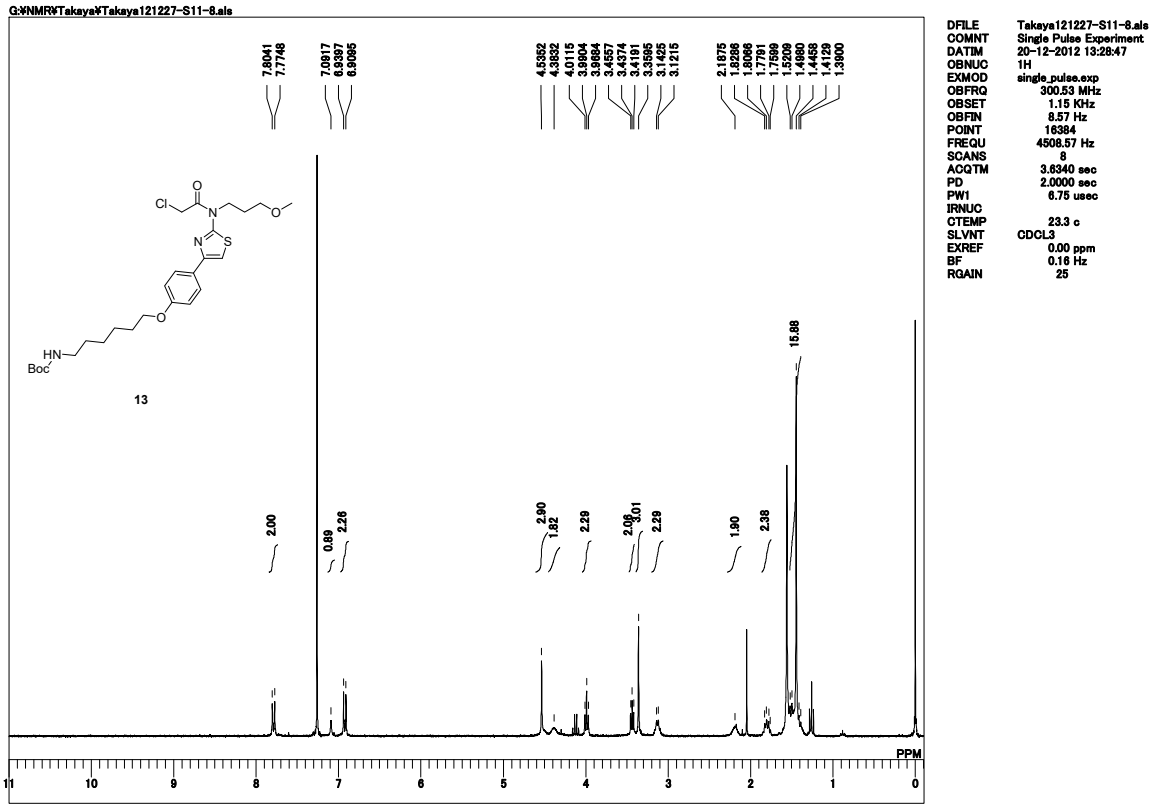

LC chart of **1**

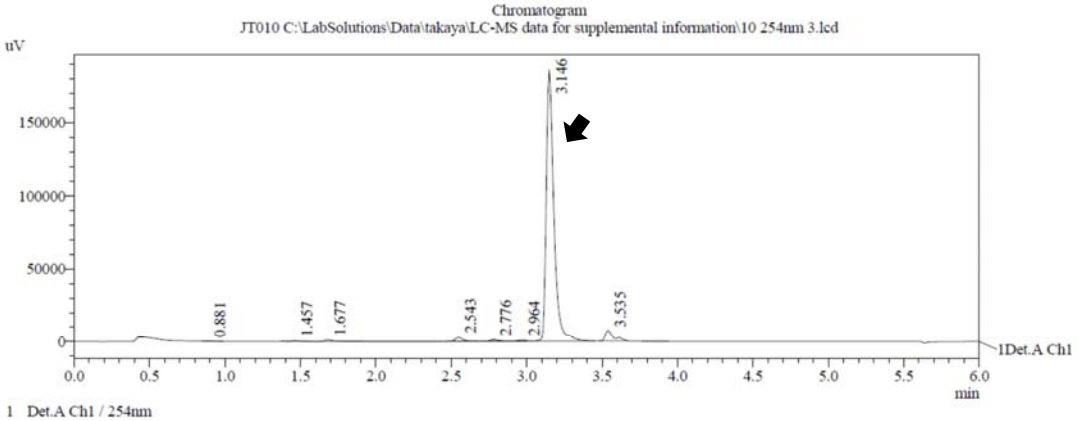

PeakTable

Detector A Ch1 254nm

Peak#	Ret. Time	Area	Height	Area %	Height %
1	0.881	521	115	0.074	0.057
2	1.457	2507	605	0.357	0.302
3	1.677	4964	1133	0.706	0.567
4	2.543	10155	2763	1.445	1.381
5	2.776	5098	1248	0.726	0.624
6	2.964	3208	897	0.457	0.449
7	3.146	648207	186109	92.247	93.054
8	3.535	28027	7132	3.988	3.566
Total		702687	200001	100.000	100.000

LC chart of **2**

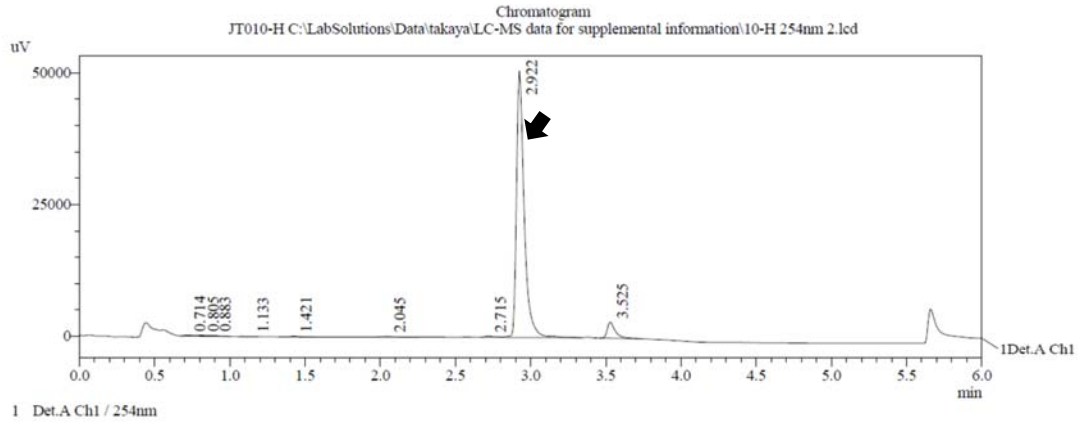

PeakTable

Detector A Ch1 254nm

Peak#	Ret. Time	Area	Height	Area %	Height %
1	0.714	552	134	0.281	0.245
2	0.805	603	140	0.307	0.257
3	0.883	675	139	0.344	0.254
4	1.133	62	17	0.032	0.031
5	1.421	657	144	0.335	0.265
6	2.045	1316	151	0.671	0.276
7	2.715	1023	253	0.521	0.464
8	2.922	179911	50622	91.644	92.716
9	3.525	11516	2998	5.866	5.491
Total		196317	54599	100.000	100.000

LC chart of **3**

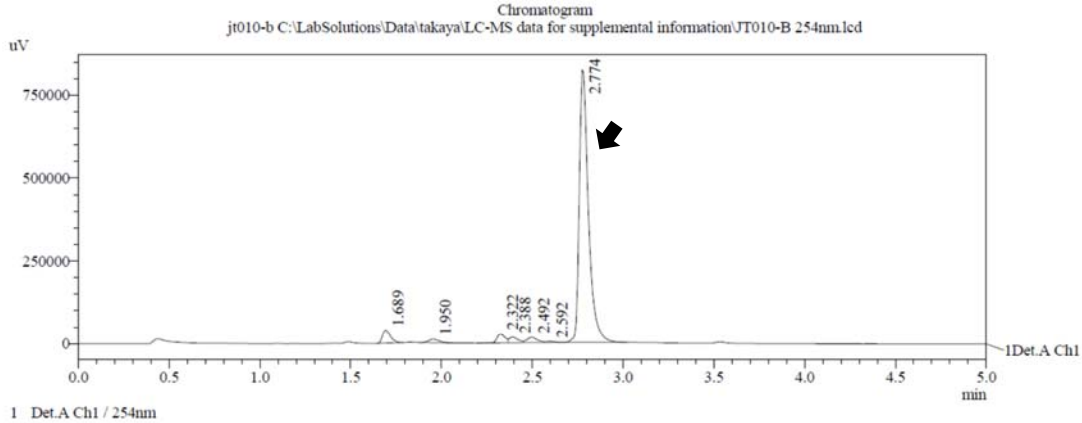

PeakTable

Detector A Ch1 254nm

Peak#	Ret. Time	Area	Height	Area %	Height %
1	1.689	123703	39972	3.773	4.258
2	1.950	44251	10968	1.350	1.168
3	2.322	88480	27563	2.698	2.936
4	2.388	56578	17613	1.726	1.876
5	2.492	65008	16392	1.983	1.746
6	2.592	10339	3333	0.315	0.355
7	2.774	2890546	822827	88.156	87.659
Total		3278905	938668	100.000	100.000